Applied Energy 228 (2018) 1071–1090

Contents lists available at ScienceDirect

Applied Energy

journal homepage: www.elsevier.com/locate/apenergy

An integrated model for estimating the techno-economic performance of the distributed solar generation system on building façades: Focused on energy demand and supply

Jeongyoon Oh[a], Choongwan Koo[b,*], Taehoon Hong[a], Seung Hyun Cha[c]

[a] Department of Architecture and Architectural Engineering, Yonsei University, Seoul 03722, Republic of Korea
[b] Department of Architectural Engineering, Kyonggi University, Suwon 16227, Republic of Korea
[c] Department of Building Services Engineering, The Hong Kong Polytechnic University, Hung Hom, Kowloon, Hong Kong

HIGHLIGHTS

- A novel approach was developed for analyzing the building energy demand and supply.
- The techno-economic performance of the DSG system on building façades was estimated.
- The finite element method was used to simplify the complex conventional approach.
- The effectiveness and efficiency of the integrated model (i-FEM) were validated.
- The usability, integrity, and practicality of the novel approach were enhanced.

ARTICLE INFO

Keywords:
Integrated model
Distributed solar generation
Building façade
Building energy demand and supply
Finite element method
Life-cycle cost analysis

ABSTRACT

There has been growing interest in the distributed solar generation (DSG) system in accordance with the 'Post-2020 Climate Change Agreement', especially for the reduction of greenhouse gas emissions from buildings. In this respect, this study aimed to develop an integrated model for estimating the techno-economic performance of the DSG system on building façades, with a focus on energy demand and supply. The integrated model was developed in five stages: (i) definition of design variables affecting the DSG system on building façades; (ii) establishment of a standard database for the DSG system on building façades using energy simulation; (iii) technical analysis of the DSG system on building façades using the finite element method; (iv) economic analysis of the DSG system on building façades through life-cycle cost analysis; and (v) systemization. Detailed analyses were conducted in three aspects: (i) nonlinearity analysis; (ii) validation of the developed model; and (iii) practical application (to the 'S' apartment block in South Korea). With the newly developed integrated model (i-FEM), it was found that the technical performance of the DSG system could be accurately estimated in only 6 s: (i) heating energy demand (1.01%); (ii) cooling energy demand (9.27%); and (iii) building energy supply (3.55%). It is expected that decision-makers (e.g. construction managers or facility managers) can use the newly developed integrated model (i-FEM) to evaluate the potential impact of the DSG system on building façades in a timely and accurate manner.

1. Introduction

At the 21st session of the Conference of Parties (COP 21) of the United Nations Framework Convention on Climate Change (UNFCCC) in Paris, France, on 9 December 2015, the United Nations (UN) sought to get agreement on a new international framework following the Kyoto Protocol. Accordingly, the '*Post-2020 Climate Change Agreement*' was launched and endorsed by 196 countries around the world [1].

The South Korean government targeted a greenhouse gas (GHG) emissions reduction of 37% by 2030, compared to business as usual (BAU). On 6 December 2016, '*The 1st Basic Plan for Response to Climate Change*' and the '*Basic National Roadmap for GHG Reductions by 2030*' were established to allocate the amount of reduction by industry. In addition, the government plans to reduce 219 million tons of GHG emissions by 2030 (i.e. 25.7% of 2030 BAU) from eight main sectors, including the reduction of 35.8 million tons from buildings [2].

* Corresponding author.
E-mail addresses: omk1500@yonsei.ac.kr (J. Oh), cwkoo@kgu.ac.kr (C. Koo), hong7@yonsei.ac.kr (T. Hong), seung-hyun.cha@polyu.edu.hk (S.H. Cha).

https://doi.org/10.1016/j.apenergy.2018.06.119
Received 13 December 2017; Received in revised form 22 June 2018; Accepted 22 June 2018
Available online 06 July 2018
0306-2619/ © 2018 Elsevier Ltd. All rights reserved.

Nomenclature

Abbreviations

BAU	business as usual
BED	building energy demand
BEDS	building energy demand and supply
BEP	break-even point
BES	building energy supply
BIPBs	building-integrated photovoltaic blinds
CIGS	copper indium gallium selenide
ESB	electricity-saving benefit
FEM	finite element method
GC plan	grid-connected utilization plan
$GC_{incl.SREC}$ plan	grid-connected utilization plan including the SREC
$GC_{excl.SREC}$ plan	grid-connected utilization plan excluding the SREC
GHG	greenhouse gas
i-FEM	integrated finite element model
IIC	initial investment cost
KCERs	Korean certified emissions reductions
KPX	Korea power exchange
LCC analysis	life cycle cost analysis
NPV	net present value
MOLIT	Ministry of Land, Infrastructure and Transport
PV	photovoltaic
SC plan	self-consumed utilization plan
SIR	saving-to-investment ratio
SMP	system marginal price
SREC	solar renewable energy certificate
UNFCCC	the united nations framework convention on climate change
VBA	visual basic for application
VT	visible transmittance
WWR	window-to-wall ratio

With respect to residential buildings in South Korea, the annual 5.8 million tons of GHG emissions derive from energy consumption during operation and maintenance, of which 58% is a consequence of the heating and cooling energy demand. This demand is closely related to building envelope design [3–6]. Accordingly, the government has proposed energy policies and design standards for systematic building envelope design: (i) '*Energy-saving design criteria for buildings*'; (ii) '*Low-carbon, green-energy building design guidelines*'; and (iii) '*Standard for the design and performance evaluation of residential green buildings*' [7–9].

To achieve the targeted reduction by 2030, it will be essential to adopt a more proactive strategy (such as new and renewable energy) along with systematic building envelope design. In particular, there has been growing interest in the distributed solar generation (DSG) system, which is easy to implement, as an alternative to existing centralized power plants [10]. The DSG system could reduce the loss of power entailed by delivering electricity generated in the centralized power plants. If the DSG system is introduced as part of the systematic building envelope design, it could become a way to realize net-zero-energy buildings. In addition, since it is required to install the new and renewable energy systems for public buildings over the minimum requirement (e.g. 18% of total energy demand in 2018, South Korea), it is inevitable to utilize the building façade as well as the rooftop when introducing the photovoltaic (PV) system to meet the requirement. In particular, it is strongly recommended by the government to install the PV system in the south facing façades of high-rise buildings in a big city (e.g. Seoul, Hong Kong) [11–15]. In order to promote the business, the Korean government provides the subsidy for the initial investment as an incentive. In this regard, this study aimed to investigate the potential impact of the DSG system on building façades (i.e., a building-integrated photovoltaic blind (BIPB) system) from the perspective of the building energy demand and supply.

Previous studies have analyzed the building energy demand and supply with difference envelope design, which can be categorized into three aspects: (i) building energy demand (BED); (ii) building energy supply (BES); and (iii) building energy demand and supply (BEDS) (see Table 1) [16–33].

First, some previous studies analyzed the techno-economic performance of different building envelope design in terms of the BED through energy simulation tools and multiple calculations. Lam et al. [16] used climate data to analyze the relationship between the overall thermal transfer value of building skins, and evaluated energy performance through the '*DOE-2*' software program. Huang et al. [17] focused on the effect of the building envelope (i.e. the insulation material and high-reflectivity coating) on cooling demand via the '*EnergyPlus*' software program. Koo et al. [18] proposed a model for predicting the BED (i.e., heating and cooling load) using the architectural and window design variables via the '*DesignBuilder v3.0*' software program. Hong et al. [19] sought to identify the optimal energy-saving technology (e.g. insulation on window frames) in terms of energy efficiency, reduction of CO_2 emissions and life-cycle cost (LCC), by using the '*DesignBuilder v2.2*' software program.

Second, other previous studies used various methods to conduct the techno-economic analysis of different building envelope design in terms of the BES through energy simulation tools and multiple calculations. Hong et al. [20] sought to visualize the optimal amount of electricity generated by the PV system and the corresponding optimal PV panel's installation angle by region, using the Geographic Information System (GIS) and genetic algorithm. Koo et al. [21] developed a model for predicting the amount of electricity generated from distributed solar generation system via the 9-node-based finite element model. Kang et al. [22] used the mathematical model to analyze the technical performance of BIPBs by considering several design variables (e.g. orientation, blind-slat angle, and standard of PV panel). Bahr [23] proposed an optimal design of BIPBs by considering the estimated amount of electricity generated from BIPBs through the '*Autodesk Ecotect analysis*' software program and the relevant results from the cost-benefit analysis.

Finally, other studies focused on the technical analysis of different building envelope design in terms of the BEDS through energy simulation tools and multiple calculations. Hachem et al. [24] analyzed the BEDS via the '*EnergyPlus*' software program by considering various design variable (e.g. density of buildings and floorplan.). Hwang et al. [25] presented the optimal design of PV systems by simultaneously considering the amount of electricity generated from PV systems and the electricity consumption through the '*e-QUEST*' and '*PV-DesignPro*' software programs. Chae et al. [26] analyzed the thermal-optical properties of commercial buildings with building-integrated PV window systems in terms of the heating and cooling energy demand and the amount of electricity generated by PV systems via the '*EnergyPlus 6.0*' and '*Equivalent one-diode*' software programs.

The limitations of the previous studies on the techno-economic performance of different building envelope design in terms of the BEDS (especially, for the DSG system) can be explained in three aspects: (i) usability; (ii) integrity; and (iii) practicality.

- *Usability:* The conventional methods (e.g., energy simulation modeling and mathematical formulas) cannot be used for a decision-maker (such as a construction manager or facility manager) to carry out the quick review of design alternatives at the early design stage. This is because the conventional methods require the detailed information (e.g., building's physical characteristics, operational schedule, equipment capacity) that can be obtained from design

Table 1
Literature review on the estimation of the building energy demand and supply.

Classification	Research	Analysis target		Impact factors			Tool
		Technical aspect	Economic aspect	Architectural design variables	Window design variables	PV (BIPB) design variables	
Building energy demand (BED)	Lam et al. [16]	O	–	Orientation, external surface finish color, radiation	Window area, glass type	–	DOE-2, linear regression equation
	Huang et al. [17]	O	–	Orientation, wall and roof physical properties, radiation	–	–	EnergyPlus
	Koo et al. [18]	O	–	Region, household size, orientation, household location	Glazing/awning type, window-to-wall ratio	–	DesignBuilder v3.0
	Hong et al. [19]	O	O	Insulator location	Window and frame type, shading effect	–	DesignBuilder v2.2
	Suh and Chang [27]	O	–	Number of households, elapse year, maintenance area, number of stories, corridor type, region	–	–	Artificial neural network
	Bojic et al. [28]	O	–	Insulator's physical properties, insulator location	–	–	HTB2
	Ouyang et al. [29]	O	O	Building layout, roof/exterior wall's thermal inertia, heat transmission, green vegetation on wall/roof	Window-to-wall ratio, window's physical properties	–	DOE-2
Building energy supply (BES)	Park et al. [15]	O	O	Region, orientation	Visible transmittance, window area	Window-to-PV panel ratio, PV panel's efficiency	Autodesk Ecotect analysis
	Hong et al. [20]	O	–	Latitude, monthly meridian altitude, solar radiation	–	The azimuth/slope of PV panel, PV panel/inverter type	RETScreen
	Koo et al. [21]	O	–	Region, orientation	Visible transmittance, window area	Window-to-PV panel ratio, PV panel's efficiency	Autodesk Ecotect analysis
	Kang et al. [22]	O	–	Weather, location, orientation	Window type, solar transmittance	Blind and PV module's Specification and angle, distance of blind from outer window	Mathematical model
Building energy supply (BES)	Bahr [23]	O	O	–	–	Ratio between the panel's installation distance and module depth, blinds angle, panel type	Autodesk Ecotect analysis
	Siraki and Pillay [30]	O	–	Location, weather conditions, surrounding buildings, radiation	–	Solar panel tilt angle	HDKR anisotropic sky model
	Cucchiella and D'Adamo [31]	O	–	Average annual insolation, Orientation	–	PV module's efficiency, active surface, PV panel's angle, balance of system, PV module's nominal power/lifetime, number of installed PV modules, tracking type	Multiple calculations
	Pillai et al. [32]	O	O	Irradiation, temperature	–	Module/inverter type, PV panel angle/installation capacity	PVSyst software
Building energy demand and supply (BEDS)	Hachem et al. [24]	O	–	Azimuth angle, orientation, building density, site layout	–	Available area for the PV integration, shading effect	EnergyPlus
	Hwang et al. [25]	O	–	Total floor area, height, wall orientation, weather	–	PV panel's angle, ratio of distance between panels and panel's length, PV panel type	e-QUEST, PV-DesignPro software
	Chae et al. [26]	O	–	Conditioned floor area, location	Glazing type, transmittance/reflectance of light, window area, window-to-wall ratio	Solar cell type	EnergyPlus 6.0, equivalent one diode
	Vettorato et al. [33]	O	–	Orientation, roof form and inclination, terrain morphology, atmospheric turbidity factor	–	Shading effect	LiDAR/household survey, vector map, meteorological data, GRASS 6.4

drawings and specifications. In addition, the conventional methods require the complex processes (e.g., developing physical model and entering detailed design properties) in investigating the technical performance of different building envelope design in terms of the BEDS, which lead to considerable time delay. Thus, the conventional methods are limited to be used for the quick review of several design alternatives in terms of the BEDS (especially, for the DSG system).

- *Integrity:* A simplified energy simulation modeling or a linear regression model was often used in the previous studies to address the aforementioned challenge (i.e., usability); however, the accuracy of the estimated values was found to be relatively low. This is because the simplified approach cannot take account of significant factors (such as shading effects or window properties) that can cause a nonlinear effect on the technical performance of different building envelope design in terms of the BEDS. Furthermore, various aspects of the BEDS should be simultaneously considered in investigating the techno-economic performance of different building envelope design; however, the previous studies rarely focused on an integrated analysis on the BEDS (especially, for the DSG system).
- *Practicality:* Due to uniqueness in building envelope design, the results from the conventional methods can be used only for the target building; however, they cannot be extended to other buildings with different properties on the building envelope design. Thus, it is required to establish the standard structure of the database for the BEDS (especially, for the DSG system) to enhance the practicality of the estimation model. In addition, it is required to analyze the economic performance of the DSG system as well as its technical performance for making better decisions in practice.

To address these challenges, a novel approach needs to be developed to overcome the limitations of the conventional methods for the investigation of the techno-economic performance of the DSG system. As a promising way, a finite element method (FEM) has the potential of improving the usability of the estimation model by simplifying the complex processes of the conventional methods. As indicated in a few recent studies, such as the building energy demand (heating and cooling load) conducted by Koo et al. [18] and the building energy supply (electricity generation from PV system) conducted by Koo et al. [21], it was proved that the estimation model developed via the FEM can be used at the early design stage in a timely manner. However, there has been limited studies in applying the FEM to simultaneously estimate the technical performance of different building envelope design in terms of the BEDS; and thus, it has not been well understood whether the FEM could be suitably used for developing the integrated model on the BEDS (especially, for the DSG system). Furthermore, it is required to validate how the newly developed model could be used for the real applications by considering the economic performance of the DSG system as well as its technical performance. Therefore, it still needs to be explored whether the FEM can serve as an alternative approach to develop an integrated model for estimating the techno-economic performance of the DSG system on a building façade, focusing on both energy demand and supply.

2. Materials and methods

Fig. 1 shows the research framework for developing the integrated model in five stages: (i) stage 1: definition of the design variables affecting the DSG system on building façades; (ii) stage 2: establishment of a standard database for the DSG system on building façades using energy simulation; (iii) stage 3: technical analysis of the DSG system on building façades using the 'finite element method'; (iv) stage 4: economic analysis of the DSG system on building façades through life-cycle cost analysis; and (v) stage 5: systemization.

2.1. Stage 1: Definition of the design variables affecting the DSG system on building façades

This study identified the design variables affecting the technical performance of the DSG system in three ways (i.e., architectural, window and BIPB design variables). In particular, the design variables on the building energy demand were defined by referring the studies conducted by Koo et al. [18] and Seo et al. [34], and the design variables on the building energy supply were defined by referring the studies conducted by Koo et al. [21] and Park et al. [15]. As shown in Table 2, the design variables affecting the technical performance of the DSG system were established as an integrated reference with the indication of the relevant targets (i.e., the BED and the BES).

2.1.1. Architectural design variables

This study classified the architectural design variables in three ways: (i) variables affecting the BEDS; (ii) variables affecting the BED; and (iii) variables affecting the BES.

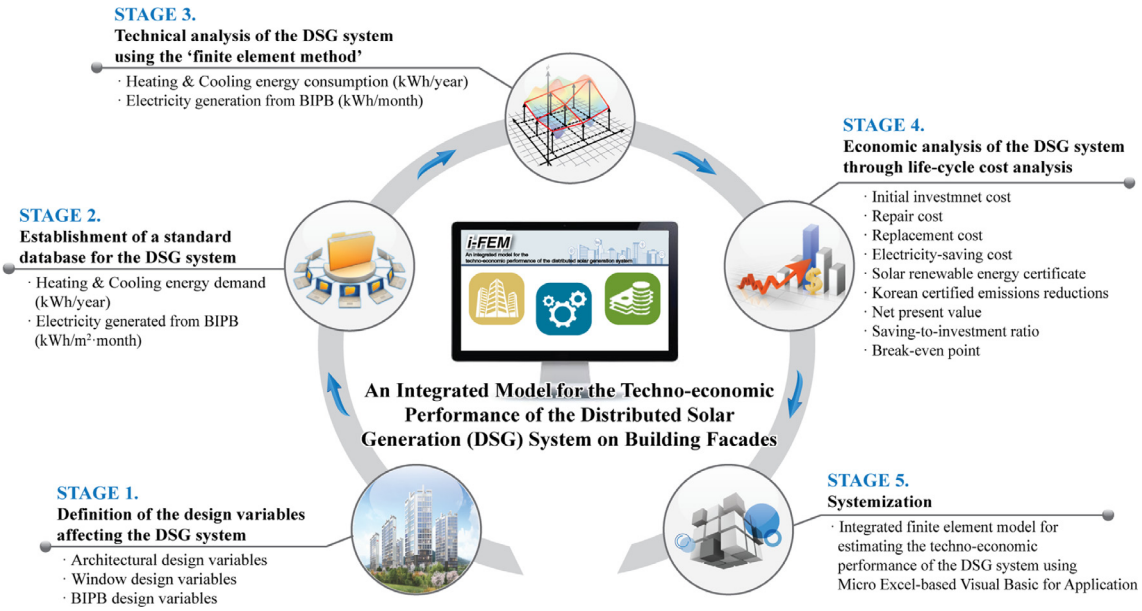
STAGE 3.
Technical analysis of the DSG system using the 'finite element method'
· Heating & Cooling energy consumption (kWh/year)
· Electricity generation from BIPB (kWh/month)
STAGE 4.
Economic analysis of the DSG system through life-cycle cost analysis
· Initial investmnet cost
· Repair cost
· Replacement cost
· Electricity-saving cost
· Solar renewable energy certificate
· Korean certified emissions reductions
· Net present value
· Saving-to-investment ratio
· Break-even point
STAGE 2.
Establishment of a standard database for the DSG system
· Heating & Cooling energy demand (kWh/year)
· Electricity generated from BIPB (kWh/m²·month)
i-FEM
An Integrated Model for the Techno-economic Performance of the Distributed Solar Generation (DSG) System on Building Facades
STAGE 1.
Definition of the design variables affecting the DSG system
· Architectural design variables
· Window design variables
· BIPB design variables
STAGE 5.
Systemization
· Integrated finite element model for estimating the techno-economic performance of the DSG system using Micro Excel-based Visual Basic for Application

Fig. 1. Research framework.

Table 2
Definition of building envelope design variables affecting the building energy demand and supply.

Classification	Attribute		Detailed classification	Type of scale	[a]Target	
					[b]BED	[c]BES
Independent variable	Architectural design variable	Region	Northern part (Seoul), central part (Daejeon), southern part (Busan)	Nominal	O	O
		Orientation	0–360°, interval: 45° (i.e., south (S): 0°, southeast (SE):45°, east (E): 90°, northeast (NE): 135°, north (N): 180°, northwest (NW): 225°, west (W): 270°, and southwest (SW): 315°)	Nominal	O	O
		Floorplan type	Type 1 (36 m^2), Type 2 (46 m^2), Type 3 (59 m^2), Type 4 (84 m^2), Type 5 (125 m^2)	Nominal	O	–
		Household location	Top floor-inside household, top floor-outside household, middle floor-inside household, middle floor-outside household, lowest floor-inside household, lowest floor-outside household	Nominal	O	–
		Exterior wall area	Value depends on the building's properties	Continuous	–	△
	Window design variable	[d]WWR	0–100%, interval: 20% (i.e., 0%, 20%, 40%, 60%, 80%, and 100%)	Nominal	O	△
		Exterior window area	Value will be calculated based on the exterior wall area and the window-to-wall ratio (WWR)	Continuous	–	O
		Glazing type	(Clr5 + Air6 + Clr5) & (Clr5 + Air6 + Clr5), (Clr5 + Air12 + Clr5) & (Clr5 + Air6 + Clr5), (Clr6 + Air12 + Clr6) & (Clr5 + Air6 + Clr5), (Clr5 + Air12 + Clr5) & (Clr5 + Air12 + Clr5), (Clr6 + Air12 + Clr6) & (Clr5 + Air12 + Clr5), (Clr6 + Air12 + Clr6) & (Clr6 + Air12 + Clr6), (Low-E Clr5 + Air12 + Clr5) & (Clr5 + Air6 + Clr5), (Low-E Clr6 + Air12 + Clr6) & (Clr5 + Air6 + Clr5), (Low-E Clr5 + Air12 + Clr5) & (Clr5 + Air12 + Clr5), (Low-E Clr5 + Air12 + Clr5) & (Clr6 + Air12 + Clr6), (Low-E Clr6 + Air12 + Clr6) & (Clr5 + Air12 + Clr5), (Low-E Clr6 + Air12 + Clr6) & (Clr6 + Air12 + Clr6), (Low-E Clr6 + Air12 + Low-E Clr5 + Air18 + Clr6)	Nominal	O	O
		Awning type	None, Curtain, Shade roll, Venetian blind (BIPB)	Nominal	O	O
		[e]VT	30–80%, interval: 10% (i.e., 30%, 40%, 50%, 60%, 70%, and 80%)	Nominal	–	O
	[f]BIPB design variable	Window-to-PV panel ratio	0–100%	Continuous	–	O
		Efficiency of PV panel	Value depends on the PV panel's properties (e.g., latest technology, up to 21.5%)	Continuous	–	O
Dependent variable	BED	Heating energy demand	Value will be estimated using the proposed model	Continuous	O	–
		Cooling energy demand	Value will be estimated using the proposed model	Continuous	O	–
	BES	Electricity generated from BIPB	Value will be estimated using the proposed model	Continuous	–	O

[a] *Note*: *Model* means the relationship between independent variables and dependent variables; *'O'* stands for the variables that have a direct effect on the BED or the BES; '△' stands for the variables that have an indirect effect on the BED or the BES; '–' stands for the variables that have no effect on the BED or the BES.
[b] *BED* stands for the building energy demand.
[c] *BES* stands for the building energy supply.
[d] *WWR* stands for the window-to-wall ratio.
[e] *VT* stands for the visible transmittance.
[f] *BIPB* stands for the building-integrated photovoltaic blind system.

- *Variables affecting the BEDS:* Two variables (i.e., 'region' and 'orientation') were determined as the architectural design variables affecting the BEDS. First, for the region as a nominal-scale variable, the northern, central, and southern parts of South Korea were considered. Second, for the orientation as a ratio-scale variable, the values within a range of 0–360° were converted into an ordinal-scale variable with eight values (i.e. South (S, 0°), Southeast (SE, 45°), East (E, 90°), Northeast (NE, 135°), North (N, 180°), Northwest (NW, 225°), West (W, 270°), and Southwest (SW, 315°)).
- *Variables affecting the BED:* Two variables (i.e., 'floorplan type' and 'household location') were determined as the architectural design variables affecting the BED. Especially, five types of the standard floorplan (i.e. Type 1 (36 m^2), Type 2 (46 m^2), Type 3 (59 m^2), Type 4 (84 m^2), and Type 5 (125 m^2)) and six household locations (i.e., Top floor-inside, top floor-outside, middle floor-inside, middle floor-outside, lowest floor-inside, and lowest floor-outside) were considered by referring the standard set by the government [35,36].
- *Variables affecting the BES:* One variable ('exterior wall area') was determined as the architectural design variables affecting the BES because it is needed to be taken into account when calculating the window area for the BIPB system along with the window-to-wall ratio (WWR).

2.1.2. Window design variables

This study classified the window design variables in two ways: (i) window design variables affecting the BEDS and (ii) window design variables affecting the BES.

- *Variables affecting the BEDS:* Three variables (i.e., 'WWR', 'glazing type', and 'awning type') were determined as the window design variables affecting the BEDS because they have effects on the solar radiation and the physical properties of windows. First, for the WWR as a ratio-scale variable, the values with a range of 0–100% were divided into an ordinal-scale variable with six values (i.e. 0%, 20%, 40%, 60%, 80%, and 100%) Second, 13 glazing types were defined through a market survey of windows in South Korea. Third,

four awning types (i.e. none, curtain, shade roll, and venetian blind (i.e., BIPB)) were considered as representative ones [37].

- *Variables affecting the BES:* Two variables (i.e., 'exterior window area' and 'visible transmittance (VT)') were determined as the window design variables affecting the BES. First, it was acknowledged that the exterior window area could be automatically calculated along with the WWR and exterior wall area. Second, for the VT as a ratio-scale variable, the values within a range of 30–80% were divided into an ordinal-scale variable with six values (i.e. 30%, 40%, 50%, 60%, 70%, and 80%).

2.1.3. BIPB design variables

Two variables (i.e., 'window-to-PV panel ratio' with a range of 0–100% and 'efficiency of PV panel' with a range of 0–21.5%) were determined as the BIPB design variables, which have a significant effect on the amount of electricity generated from BIPB in terms of the BES.

2.2. Stage 2: Establishment of a standard database for the DSG system on building façades using energy simulation

As an energy simulation tool, the '*DesignBuilder v3.0*' and '*Autodesk Ecotect analysis*' software programs were used to establish the standard database for the DSG system on building façades, to which the design variables set in Stage 1 were applied. That is, two types of the reference models were firstly developed for the BED and the BES, respectively. Thereafter, the reference models were used to establish a standard database for the DSG system (i.e., two types of the standard databases for the BED and the BES), in which the standard structure of the database was considered to enhance the practicality of the estimation model. That is, the standard structure of the database can be used as a finite element mesh in developing the estimation model via the FEM in Stage 3, which can affect the extendability of the developed model.

2.2.1. Definition of the reference model

Two types of the reference models (i.e., for the BED and the BES) were developed via energy simulation tool, which can be used for establishing the relevant standard databases.

- *Reference model for the BED:* The reference model was developed by considering three variables via the '*DesignBuilder v3.0*' software program. First, three regions (i.e., northern, central, and southern) were considered, and the southern part (Busan) was used for the validation process in Section 3.3. Second, five types of floorplan (i.e. Type 1 (36 m^2), Type 2 (46 m^2), Type 3 (59 m^2), Type 4 (84 m^2), and Type 5 (125 m^2)) were considered, and Type 5 (125 m^2) was used for the validation process in Section 3.3. Third, the building operation schedule was determined by referring the data (such as the number of appliances and the hours of use) collected from 4000 households across all regions of South Korea [38]. Meanwhile, the feasibility of the reference model was verified through the tolerance limit (i.e. CV(RMSE), 25%—for which see the Supplementary Data (SD) Equation S1) [39]. The CV(RMSE)s for the heating (i.e. gas) and cooling (i.e. electricity) energy consumption were determined as 6.25% and 14.26% respectively (for which see SD Fig. S1).
- *Reference model for the BES:* The reference model was developed by considering three variables via the '*Autodesk Ecotect analysis*' software program. First, for the size of reference model, 100% of the window-to-PV panel ratio was applied to the 1 m^2 of window (1000 mm × 1000 mm). Second, for the standard type of a venetian blind, the depth and interval of the slat were set to 50 mm; and then, the distance between the centerline of the PV panel and the exterior window was set to 25 mm [40,41]. Third, for the type of a PV panel, the copper indium gallium selenide (CIGS) with 11.70% efficiency was determined in this study.

2.2.2. Establishment of the standard database

Based on the established reference models, two types of the standard databases were established for the BED and the BES.

- *Standard database for the BED:* In establishing the standard database for the BED (i.e. heating and cooling energy demand (2 types)), five nominal-scale design variables were considered: (i) orientation (8 types); (ii) household location (6 types); (iii) glazing type (13 types); (iv) awning type (4 types); and (v) WWR (6 types). In this way, the standard database for the BED was established with a total of 29,952 (2 × 8 × 6 × 13 × 4 × 6) data-points (for which see SD Tables S1-S2).
- *Standard database for the BES:* In establishing the standard database for the BES (i.e. the amount of electricity generated by BIPB per unit area), three nominal-scale design variables were considered: (i) region (3 locations); (ii) orientation (8 types); and (iii) VT (6 types). As the amount of electricity generated from BIPB was analyzed on a monthly basis (12 months), the standard database for the BES was established with a total of 1728 (3 × 8 × 6 × 12) data-points (for which see SD Table S3).

Design variable	*Code*	*Detailed description*
Region	R	R_1~R_3 (ex: R_3 stands for Southern part (Busan))
Orientation	O	0~360° —*Discretization Interval: 45°*→ O_1~O_8 (ex: O_1 stands for South (0°))
Floorplan type	F	F_1~F_5 (ex: F_5 stands for Type 5 (125m^2))
Household location	H	H_1~H_6 (ex: H_3 stands for middle floor-inside household)
Window-to-wall ratio	WW	0~100% —*Discretization Interval: 20%*→ WW_1~WW_6 (ex: WW_3 stands for 40%)
Glazing type	G	G_1~G_{12} (ex: G_1 stands for (Clr5+Air6+Clr5)&(Clr5+Air6+Clr5))
Awning type	A	A_1~A_4 (ex: A_4 stands for venetian blind (BIPB))
Breakdown structure code: R_3-O_1-F_5-H_3-WW_3-G_1-A_4		

Fig. 2. Breakdown structure for establishing ξ (orientation) – η (WWR) matrix for the building energy demand (BED).

2.3. Stage 3: Technical analysis of the DSG system on building façades using the 'finite element method'

With the standard database set in Stage 2, the FEM was used to estimate the technical performance of the DSG system on building façade (i.e., two types of the estimation model for the BED and the BES). The estimation process can be explained in three steps: (i) selection of design variables applicable to FEM; (ii) discretization of continuous-scale design variables; and (iii) determination of the shape and interpolation function.

2.3.1. Selection of the design variables applicable to FEM

The design variables applicable to FEM were determined by model (for the BED and the BES), and they were used for developing the finite element mesh.

- *Design variables applicable to FEM for the BED:* Among the seven design variables (i.e. region, orientation, floorplan type, household location, WWR, glazing type, and awning type) that were considered in establishing the standard database for the BED, two variables (i.e., 'orientation' and 'WWR') were on ratio scales with ranges of 0–360° and 0–100%, respectively. Since these two variables were analyzed to have a nonlinear effect on the heating and cooling energy demand (see Section 3.1), this study selected the orientation (ξ) and WWR (η) as appropriate design variables to be used for FEM.
- *Design variables applicable to FEM for the BES:* Among the eight design variables (i.e., region, orientation, exterior window area, glazing type, awning type, VT, window-to-PV panel ratio, and efficiency of PV panel) that were considered in establishing the standard database for the BES, two variables (i.e., 'orientation' and 'VT') were on ratio scales with ranges of 0–360° and 30–80%, respectively. Since these two variables were analyzed to have a nonlinear effect on the amount of electricity generated from BIPB (see Section 3.1), this study selected the orientation (ξ) and VT (η) as appropriate design variables to be used for FEM.

2.3.2. Discretization of continuous-scale design variables

Based on the selected design variables applicable to FEM, this study discretized the continuous variables.

- *Discretization of variables for the BED:* The discretization of the design variables ξ (orientation) and η (WWR) applicable to FEM was undertaken so that eight points of the orientations (0–360° by 45° intervals) and six points of the WWRs (0–100% by 20% intervals) were established. Fig. 2 shows the breakdown structure for establishing the ξ-η matrix for the BED. In addition, SD Tables S4 and S5 show the examples of the ξ-η matrix for the heating and cooling energy demand in the FEM depending on the discretized variables (i.e., orientation and WWR).
- *Discretization of variables for the BES:* The discretization of design variables ξ (orientation) and η (VT) applicable to FEM was carried out so that eight points of the orientations (0–360° by 45° intervals) and six points of the VTs (30–80% by 10% intervals) were established. Fig. 3 shows the breakdown structure for establishing the ξ-η matrix for the BES. In addition, SD Table S6 shows the example of the ξ-η matrix for the amount of electricity generated from BIPB in the FEM depending on the discretized variables (i.e., orientation and VT).

2.3.3. Determination of the shape and interpolation function

Using the ξ-η matrix, the shape and interpolation function can be determined to estimate the technical performance of the DSG system on building façades by model (for the BED and the BES). In this process, the building envelope design can be reflected by taking account of the key design variables (i.e., orientation, WWR, and VT).

First, the shape function was determined in three steps: (i) variable configuration; (ii) function configuration; and (iii) determination of shape function.

- *Variable configuration:* The design variables applicable to FEM were determined by model (for the BED and the BES). For the BED, ξ and η were determined to be the orientation and WWR, respectively. For the BES, ξ and η were determined to be orientation and VT, respectively.
- *Function configuration:* For the BED, $\phi(\xi, \eta)$ was defined as the heating and cooling energy demand with regard to the orientation (ξ) and WWR (η). For the BES, $\phi(\xi, \eta)$ was defined as the amount of electricity generated by BIPB in response to orientation (ξ) and VT (η).
- *Shape function:* Based on the results from the variable configuration (ξ, η) and function configuration ($\phi(\xi, \eta)$), the shape function can be determined with nine extreme points. Equation (1) shows the nine-node-based *Lagrangian* shape function based on Pascal's triangle (see Fig. 4 and SD Fig. S2).

$$\phi(\xi, \eta) = \alpha_1 \cdot \xi + \alpha_2 \cdot \xi^2 + \alpha_3 \cdot \xi^2 \cdot \eta + \alpha_4 \cdot \xi^2 \cdot \eta^2 + \alpha_5 \cdot \xi \cdot \eta^2 + \alpha_6 \cdot \eta^2 + \alpha_7 \cdot \eta + \alpha_8 \cdot \xi \cdot \eta + \alpha_9 \quad (1)$$

where variables and the relevant functions depend on the analysis target (whether BED or BES) and α_1–α_9 stands for the coefficient of the nine-node-based *Lagrangian* shape function.

Second, the nine polynomial expressions can be generated by applying the values at the nine points in the ξ-η matrix to the general expression of the shape function (see Eq. (1)). Using the nine polynomial expressions, the interpolation function can be determined as shown in Eq. (2). Also, as shown in Eq. (3), the inverse matrix can be used to find the coefficient of a nine-node-based *Lagrangian* shape function.

Design variable	Code	Detailed description
Region	R	R_1~R_3 (ex: R_3 stands for Southern part (Busan))
Orientation	O	0~360° —Discretization Interval: 45°→ O_1~O_8 (ex: O_1 stands for South (0°))
Exterior window area	E	E_0~E_∞(ex: E_1 stands for 1m²)
Visible transmittance	V	30~80% —Discretization Interval: 10%→ V_1~V_6 (ex: V_5 stands for 70%)
Window-to-**P**V panel ratio	WP	WP_0~WP_{100} (ex: WP_{100} stands for 100%)
Efficiency of **P**V panel	EP	EP_0~$EP_{21.5}$ (ex: $EP_{11.70}$ stands for 11.70%)
Breakdown structure code: R_3-O_1-E_1-V_5-WP_{100}-$EP_{11.70}$		

Fig. 3. Breakdown structure for establishing ξ (orientation) – η (VT) matrix for the building energy supply (BES).

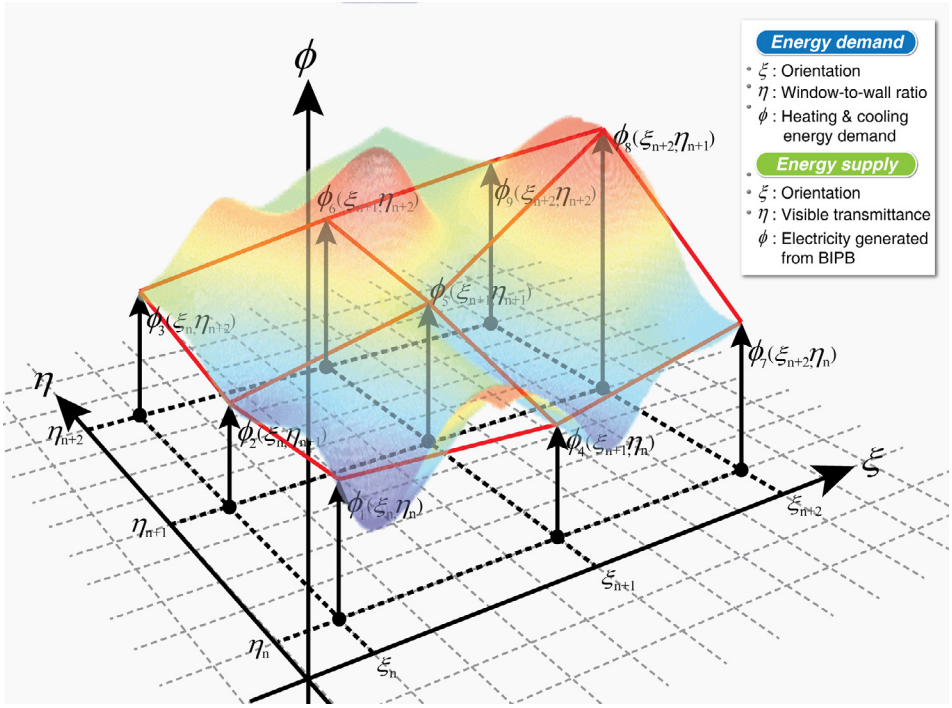

Fig. 4. Concept of the nine-node-based *Lagrangian* shape function.

For the BED, a total of 624 $\xi - \eta$ matrices [4 (awning type) × 13 (glazing type) × 6 (household location) × 2 (heating and cooling energy demand)] can be generated. The $\xi - \eta$ matrix also consists of a total of 48 data-points [8 (orientation) × 6 (WWR)]. Thus, a total of 29,952 (624 × 48) shape and interpolation functions can be developed for estimating the heating and cooling energy demand (see SD Tables S4-S5). Meanwhile, from the BES, a total of 36 $\xi - \eta$ matrices [12 (month) × 3 (region)] can be generated. The $\xi - \eta$ matrix also consists of a total of 48 data-points [8 (orientation) × 6 (VT)]. Thus, a total of 1728 (36 × 48) shape and interpolation functions can be developed for investigating the amount of electricity generated from BIPB (see SD Table S6). As a result, a total of 31,680 shape and interpolation functions [29,952 (for the BED) + 1728 (for the BES)] can be generated to carry out the integrated analysis for both the BED and the BES.

where variables and the relevant functions depend on the analysis target (whether it is BED or BES). In terms of the BED, ϕ stands for the heating and cooling energy demand; ξ stands for the orientation; and η stands for the window-to-wall ratio (WWR). In terms of the BES, ϕ stands for the amount of electricity generated from BIPB; ξ stands for the orientation; and η stands for the visible transmittance (VT). α_1–α_9 stands for the coefficient of the nine-node-based *Lagrangian* shape function.

2.4. Stage 4: Economic analysis of the DSG system on building façades through life-cycle cost analysis

Based on the technical analysis performed in State 3, a life-cycle cost (LCC) analysis was undertaken to evaluate the economic performance of the DSG system, together with a policy analysis, which can support for better making-decisions in practice.

$$\begin{bmatrix} \xi_n & \xi_n^2 & \xi_n^2\cdot\eta_n & \xi_n^2\cdot\eta_n^2 & \xi_n\cdot\eta_n^2 & \eta_n^2 & \eta_n & \xi_n\cdot\eta_n & 1 \\ \xi_n & \xi_n^2 & \xi_n^2\cdot\eta_{n+1} & \xi_n^2\cdot\eta_{n+1}^2 & \xi_n\cdot\eta_{n+1}^2 & \eta_{n+1}^2 & \eta_{n+1} & \xi_n\cdot\eta_{n+1} & 1 \\ \xi_n & \xi_n^2 & \xi_n^2\cdot\eta_{n+2} & \xi_n^2\cdot\eta_{n+2}^2 & \xi_n\cdot\eta_{n+2}^2 & \eta_{n+2}^2 & \eta_{n+2} & \xi_n\cdot\eta_{n+2} & 1 \\ \xi_{n+1} & \xi_{n+1}^2 & \xi_{n+1}^2\cdot\eta_n & \xi_{n+1}^2\cdot\eta_n^2 & \xi_{n+1}\cdot\eta_n^2 & \eta_n^2 & \eta_n & \xi_{n+1}\cdot\eta_n & 1 \\ \xi_{n+1} & \xi_{n+1}^2 & \xi_{n+1}^2\cdot\eta_{n+1} & \xi_{n+1}^2\cdot\eta_{n+1}^2 & \xi_{n+1}\cdot\eta_{n+1}^2 & \eta_{n+1}^2 & \eta_{n+1} & \xi_{n+1}\cdot\eta_{n+1} & 1 \\ \xi_{n+1} & \xi_{n+1}^2 & \xi_{n+1}^2\cdot\eta_{n+2} & \xi_{n+1}^2\cdot\eta_{n+2}^2 & \xi_{n+1}\cdot\eta_{n+2}^2 & \eta_{n+2}^2 & \eta_{n+2} & \xi_{n+1}\cdot\eta_{n+2} & 1 \\ \xi_{n+2} & \xi_{n+2}^2 & \xi_{n+2}^2\cdot\eta_n & \xi_{n+2}^2\cdot\eta_n^2 & \xi_{n+2}\cdot\eta_n^2 & \eta_n^2 & \eta_n & \xi_{n+2}\cdot\eta_n & 1 \\ \xi_{n+2} & \xi_{n+2}^2 & \xi_{n+2}^2\cdot\eta_{n+1} & \xi_{n+2}^2\cdot\eta_{n+1}^2 & \xi_{n+2}\cdot\eta_{n+1}^2 & \eta_{n+1}^2 & \eta_{n+1} & \xi_{n+2}\cdot\eta_{n+1} & 1 \\ \xi_{n+2} & \xi_{n+2}^2 & \xi_{n+2}^2\cdot\eta_{n+2} & \xi_{n+2}^2\cdot\eta_{n+2}^2 & \xi_{n+2}\cdot\eta_{n+2}^2 & \eta_{n+2}^2 & \eta_{n+2} & \xi_{n+2}\cdot\eta_{n+2} & 1 \end{bmatrix} \begin{bmatrix} \alpha_1 \\ \alpha_2 \\ \alpha_3 \\ \alpha_4 \\ \alpha_5 \\ \alpha_6 \\ \alpha_7 \\ \alpha_8 \\ \alpha_9 \end{bmatrix} = \begin{bmatrix} \phi_1(\xi_n, \eta_n) \\ \phi_2(\xi_n, \eta_{n+1}) \\ \phi_3(\xi_n, \eta_{n+2}) \\ \phi_4(\xi_{n+1}, \eta_n) \\ \phi_5(\xi_{n+1}, \eta_{n+1}) \\ \phi_6(\xi_{n+1}, \eta_{n+2}) \\ \phi_7(\xi_{n+2}, \eta_n) \\ \phi_8(\xi_{n+2}, \eta_{n+1}) \\ \phi_9(\xi_{n+2}, \eta_{n+2}) \end{bmatrix} \tag{2}$$

$$\begin{bmatrix} \alpha_1 \\ \alpha_2 \\ \alpha_3 \\ \alpha_4 \\ \alpha_5 \\ \alpha_6 \\ \alpha_7 \\ \alpha_8 \\ \alpha_9 \end{bmatrix} = \begin{bmatrix} \xi_n & \xi_n^2 & \xi_n^2\cdot\eta_n & \xi_n^2\cdot\eta_n^2 & \xi_n\cdot\eta_n^2 & \eta_n^2 & \eta_n & \xi_n\cdot\eta_n & 1 \\ \xi_n & \xi_n^2 & \xi_n^2\cdot\eta_{n+1} & \xi_n^2\cdot\eta_{n+1}^2 & \xi_n\cdot\eta_{n+1}^2 & \eta_{n+1}^2 & \eta_{n+1} & \xi_n\cdot\eta_{n+1} & 1 \\ \xi_n & \xi_n^2 & \xi_n^2\cdot\eta_{n+2} & \xi_n^2\cdot\eta_{n+2}^2 & \xi_n\cdot\eta_{n+2}^2 & \eta_{n+2}^2 & \eta_{n+2} & \xi_n\cdot\eta_{n+2} & 1 \\ \xi_{n+1} & \xi_{n+1}^2 & \xi_{n+1}^2\cdot\eta_n & \xi_{n+1}^2\cdot\eta_n^2 & \xi_{n+1}\cdot\eta_n^2 & \eta_n^2 & \eta_n & \xi_{n+1}\cdot\eta_n & 1 \\ \xi_{n+1} & \xi_{n+1}^2 & \xi_{n+1}^2\cdot\eta_{n+1} & \xi_{n+1}^2\cdot\eta_{n+1}^2 & \xi_{n+1}\cdot\eta_{n+1}^2 & \eta_{n+1}^2 & \eta_{n+1} & \xi_{n+1}\cdot\eta_{n+1} & 1 \\ \xi_{n+1} & \xi_{n+1}^2 & \xi_{n+1}^2\cdot\eta_{n+2} & \xi_{n+1}^2\cdot\eta_{n+2}^2 & \xi_{n+1}\cdot\eta_{n+2}^2 & \eta_{n+2}^2 & \eta_{n+2} & \xi_{n+1}\cdot\eta_{n+2} & 1 \\ \xi_{n+2} & \xi_{n+2}^2 & \xi_{n+2}^2\cdot\eta_n & \xi_{n+2}^2\cdot\eta_n^2 & \xi_{n+2}\cdot\eta_n^2 & \eta_n^2 & \eta_n & \xi_{n+2}\cdot\eta_n & 1 \\ \xi_{n+2} & \xi_{n+2}^2 & \xi_{n+2}^2\cdot\eta_{n+1} & \xi_{n+2}^2\cdot\eta_{n+1}^2 & \xi_{n+2}\cdot\eta_{n+1}^2 & \eta_{n+1}^2 & \eta_{n+1} & \xi_{n+2}\cdot\eta_{n+1} & 1 \\ \xi_{n+2} & \xi_{n+2}^2 & \xi_{n+2}^2\cdot\eta_{n+2} & \xi_{n+2}^2\cdot\eta_{n+2}^2 & \xi_{n+2}\cdot\eta_{n+2}^2 & \eta_{n+2}^2 & \eta_{n+2} & \xi_{n+2}\cdot\eta_{n+2} & 1 \end{bmatrix}^{-1} \begin{bmatrix} \phi_1(\xi_n, \eta_n) \\ \phi_2(\xi_n, \eta_{n+1}) \\ \phi_3(\xi_n, \eta_{n+2}) \\ \phi_4(\xi_{n+1}, \eta_n) \\ \phi_5(\xi_{n+1}, \eta_{n+1}) \\ \phi_6(\xi_{n+1}, \eta_{n+2}) \\ \phi_7(\xi_{n+2}, \eta_n) \\ \phi_8(\xi_{n+2}, \eta_{n+1}) \\ \phi_9(\xi_{n+2}, \eta_{n+2}) \end{bmatrix} \tag{3}$$

2.4.1. Economic analysis

For the LCC analysis, the main assumptions were defined as follows: (i) analysis approach; (ii) starting point; (iii) analysis period; (iv) real discount rate; and (v) significant costs of ownership (see Table 3) [42–51]. Economic viability can be evaluated with three measures (i.e., net present value (NPV), saving-to-investment ratio (SIR), and break-even point (BEP)). In general, if 'NPV ≥ 0' or 'SIR ≥ 1', it is deemed economically feasible (see SD Equations (S2)-(S5)).

2.4.2. Policy analysis

The policy analysis was undertaken to evaluate the economic viability depending on three utilization plans with regard to the amount of electricity generated by BIPB [42–45]: (i) a self-consumed utilization plan (SC plan); (ii) a grid-connected utilization plan including the SREC ($GC_{incl.SREC}$ plan); and (iii) a grid-connected utilization plan excluding the SREC ($GC_{excl.SREC}$ plan). First, for the SC plan, the economic performance was evaluated by calculating the electricity-saving benefit (ESB), i.e., the benefit acquired by utilizing the amount of electricity generated from BIPBs. Second, for the $GC_{incl.SREC}$ plan, this study calculated the profit to be made by selling the electricity generated from BIPBs through the Korea Power Exchange (KPX), which considered both the system marginal price (SMP) and the solar renewable energy certificate (SREC). For the $GC_{excl.SREC}$ plan, the SMP was considered but the SREC was not considered.

2.5. Stage 5: Systemization

As mentioned above, various types of significant factors and the relevant complex relations should be considered in estimating the techno-economic performance of the DSG system. Since it would cause time-consuming and labour-intensive, a series of processes was systemized by using '*Microsoft Excel-based Visual Basic for Application (VBA)*'. The developed system (i.e., the integrated Finite Element Model for estimating the techno-economic performance of the DSG system, '*i-FEM*') has four parts: (i) variable selection; (ii) LCC assumption; (iii) technical analysis; and (iv) economic analysis.

- *Variable selection:* Part (1-1) of the i-FEM was designed for determining the values of design variables. First, the nominal-scale variables (e.g., region, floorplan type, household location) can be determined from a combo-box. Second, the continuous-scale variables, including the design variables applicable to FEM (i.e., orientation, WWR, and VT), can be directly entered. In Part (1-2), the efficiency and loss ratio of HVAC equipment can be selected from a combo-box to calculate the heating and cooling energy consumption from the heating and cooling energy demand estimated by the i-FEM

Table 3
Main assumptions for the LCC analysis.

Classification			Detailed description		
Analysis Approach			Present worth method		
Starting point of analysis			2017		
Analysis period			25 years		
Real discount rate	Inflation rate		3.30%		
	Electricity price growth rate		0.66%		
	Gas price growth rate		0.11%		
	CO_2 emissions trading price growth rate		2.66%		
Significant costs of ownership	Costs	[a]IIC	– Window unit price (Clr5 + Air6 + Clr5)&(Clr5 + Air6 + Clr5): 46.07 US$/m^2, (Clr5 + Air12 + Clr5)&(Clr5 + Air6 + Clr5): 51.62 US$/m^2, (Clr6 + Air12 + Clr6)&(Clr5 + Air6 + Clr5): 55.66 US$/m^2, (Clr5 + Air12 + Clr5)&(Clr5 + Air12 + Clr5): 57.18 US$/m^2 (Clr6 + Air12 + Clr6)&(Clr5 + Air12 + Clr5): 61.21 US$/m^2, (Clr6 + Air12 + Clr6)&(Clr6 + Air12 + Clr6): 65.24 US$/m^2 (Low-E Clr5 + Air12 + Clr5)&(Clr5 + Air6 + Clr5): 66.50 US$/m^2, (Low-E Clr6 + Air12 + Clr6)&(Clr5 + Air6 + Clr5):71.16 US$/m^2 (Low-E Clr5 + Air12 + Clr5)&(Clr5 + Air12 + Clr5): 72.06 US$/m^2, (Low-E Clr5 + Air12 + Clr5)&(Clr6 + Air12 + Clr6): 76.09 US$/m^2 (Low-E Clr6 + Air12 + Clr6)&(Clr5 + Air12 + Clr5): 80.75 US$/m^2, (Low-E Clr6 + Air12 + Clr6)&(Clr6 + Air12 + Clr6): 96.25 US$/m^2 (Low-E Clr6 + Air12 + Low-E Clr5 + Air18 + Clr6): 90.83 US$/m^2 – Awning: 11.78 US$/m^2 (Curtain), 12.55 US$/m^2 (Shade roll), 16.13 US$/m^2 (Venetian blind) – [b]CIGS PV panel in [c]BIPB: 268.14 US$/m^2		
		Repair cost	0.5% of IIC of BIPB (CIGS PV panel) per year		
		Replacement cost	100% of IIC of awning (Curtain, shade roll, venetian blind) per seven years		
	Benefits	Utilization plan	[d]SC plan	[e]$GC_{incl.SREC}$ plan	[f]$GC_{excl.SREC}$ plan
		[g]ESB	Under 200 kWh: 0.082 US$, 201–400 kWh: 0.162 US$, Over 400 kWh: 0.243 US$	–	–
		[h]SMP	–	0.079 US$/kWh (Jeju), 0.066 US$/kWh (other cities)	0.079 US$/kWh (Jeju), 0.066 US$/kWh (other cities)
		[i]SREC	–	78.861 US$/SREC (Jeju), 110.331 US$/SREC (other cities)	–
		[j]KCERs	9.21 US$/t$CO_2$eq	9.21 US$/t$CO_2$eq	9.21 US$/t$CO_2$eq

[a] *IIC* stands for the initial investment cost.
[b] *CIGS* stands for the copper-indium-selenide.
[c] *BIPB* stands for the building-integrated photovoltaic blind system.
[d] *SC* plan stands for the self-consumed utilization plan.
[e] $GC_{incl.SREC}$ plan stands for the grid-connected utilization plan including the SREC.
[f] $GC_{excl.SREC}$ plan stands for the grid-connected utilization plan excluding the SREC.
[g] *ESB* stands for the electricity-saving benefit.
[h] *SMP* stands for the system marginal price.
[i] *SREC* stands for the solar renewable energy certificate.
[j] *KCERs* stands for the Korean certified emissions reductions; and the exchange rate is 1145.50 won to a US $ (as at August 12, 2017).

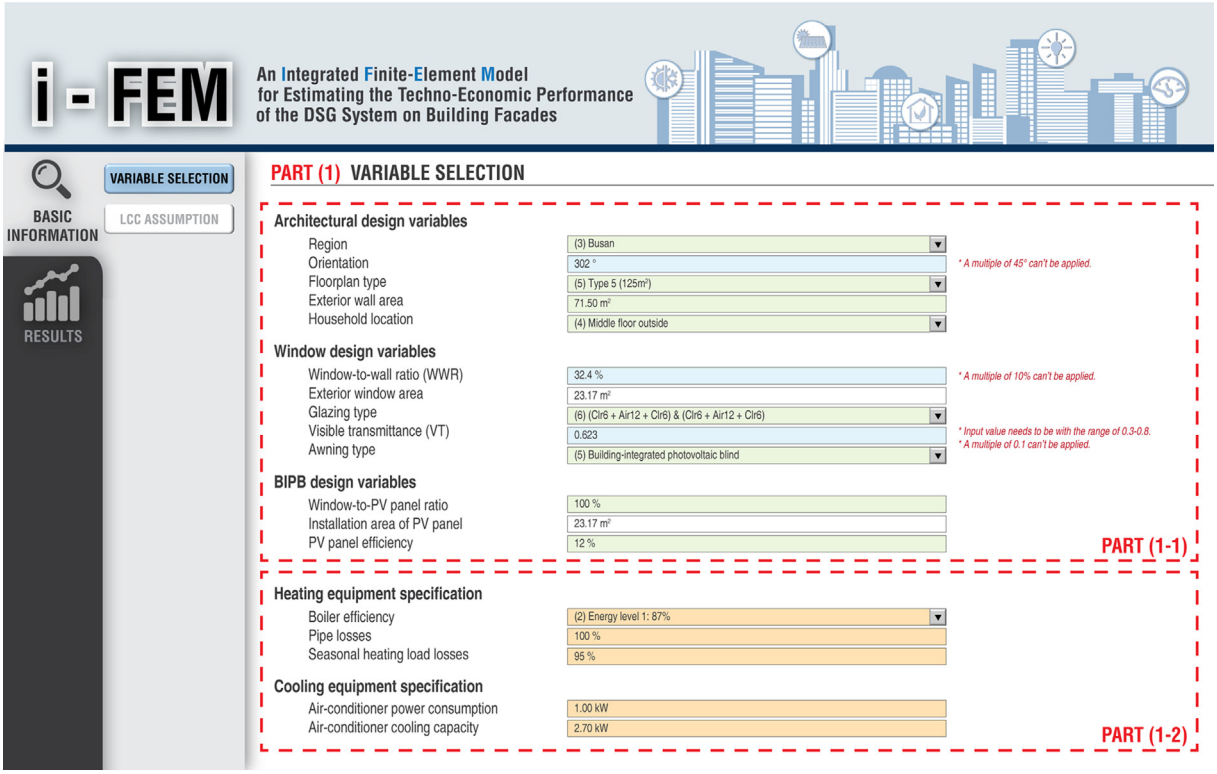

Fig. 5. Graphic user interface of the i-FEM Part 1: Variable selection.

(See Fig. 5).

- *LCC assumption:* The basic information required for the LCC analysis can be entered to analyze the economic performance of the DSG system (see Table 3). In particular, the significant price information (e.g., SMP, SREC price) can be established to conduct the policy analysis (See Fig. 6).
- *Technical analysis:* Once the basic information has been confirmed in Part (1), the technical analysis can be carried out in Part (3). First, the nine extreme points from the ξ-η matrix can be automatically determined after determining the design variables (orientation, WWR, and VT) in Part (1). Next, using the nine extreme points, the estimation process can be conducted via the shape and interpolation function. In Part (3-1) of the i-FEM, the estimated values for the heating and cooling energy consumption can be obtained. In Part (3-2) of the i-FEM, the estimated values for the monthly amount of electricity generated by BIPB can be obtained with the optimal slat's angle of BIPBs (See Fig. 7).
- *Economic analysis:* With the basic information established in Part (2) and the analysis of technical performance in Part (3), the economic analysis can be undertaken in Part (4). Parts (4-1) and (4-2) can deliver the results of the economic analysis in terms of the BED and the BES, respectively. In particular, the economic viability can be analyzed in terms of three utilization plans (i.e., the SC plan, the $GC_{incl.SREC}$ plan, and the $GC_{excl.SREC}$ plan) (See Fig. 8).

3. Results and discussion

Detailed analyses were conducted to evaluate the feasibility of the i-FEM in three ways: (i) nonlinearity analysis between the building energy demand and supply; (ii) validation of the developed model; and (iii) practical application (in the first instance, to the 'S' apartment block in South Korea).

3.1. Nonlinearity analysis between building energy demand and supply

Building energy demand and supply can be affected by various key design variables (e.g. season, orientation, WWR). These variables work together to create a thermally comfortable indoor environment. Especially, the amount of solar radiation reaching building façades depends on those factors, which can significantly affect variation in the building energy demand (heating and cooling energy demand) and the energy supply (electricity generation by BIPBs). This study demonstrates the complex and nonlinear effects of key design variables upon the technical performance of the DSG system, focusing on energy demand and supply. This nonlinearity analysis was conducted by season because South Korea is located in the monsoon climatic area (with a cold winter: low-sun season and a hot summer: high-sun season). With the nonlinearity analysis, it was demonstrated that the key design variables were appropriate for use in developing the estimation model via FEM so that the complex conventional approach could be simplified to enhance the usability of the developed model.

3.1.1. Nonlinearity analysis in the winter (or low-sun) season

Fig. 9 shows the visualized distribution of heating energy demand and the amount of electricity generated from BIPBs during the winter months (December, January and February), in which two key design variables (i.e., orientation (ξ: x axis) and WWR (η: y axis)) were mainly considered. The winter distribution was found to be nonlinear; and the detailed analyses were conducted in two parts: (i) orientation and (ii) WWR.

- *Orientation (ξ: x axis)*: As shown in Fig. 9, when the orientation was changed from north (N) to south (S), the heating energy demand tended to reduce (see a(1) and a(2) in Fig. 9), and the amount of electricity generated by BIPBs tended to increase (see b(1), b(2), c(1), c(2), d(1), and d(2) in Fig. 9). The change was attributable to the increase in heat gain from solar radiation [52]. In other words,

since Busan is located in the south of South Korea (at a latitude of 37.3°), the daily solar altitude in winter varies between 0° and 29.20° (= 90°–37.3°–23.5°). Accordingly, in a south-facing building, the winter sunlight enters throughout the day (which leads to a reduction in heating energy demand and an increase in the amount of electricity generated by BIPBs). In addition, there is no shading effect (leading to a reduction in electricity generated by BIPBs).

- *WWR (η: y axis)*: In general, the U-value of the window and its solar heat-gain coefficient are higher than those of the wall. Accordingly, as the WWR increases, the heat loss due to heat transmission increases (which causes an increase in heating energy demand), and the heat gain due to solar radiation also increases (causing a reduction in heating energy demand and an increase in electricity generation from BIPBs). As a result, in the south, as the WWR increases, the heating energy demand sharply declines (see a(1) and a(2) in Fig. 9), and the amount of electricity generated from BIPBs sharply increases (see b(1), b(2), c(1), c(2), d(1), and d(2) in Fig. 9). Meanwhile, in the north, the changes appear to be very small.

3.1.2. Nonlinearity analysis in the summer (or high-sun) season

Fig. 10 shows the visualized distribution of cooling energy demand and the amount of electricity generated from BIPBs during the summer months (June, July and August), in which two key design variables (i.e., orientation (ξ: x axis) and WWR (η: y axis)) were mainly considered. The distribution in the summer season was found to be nonlinear, and the detailed analyses were conducted in two parts: (i) orientation and (ii) WWR.

- *Orientation (ξ: x axis)*: As shown in Fig. 10, while the orientation changes from north (N) to south (S), the cooling energy demand tends to increase (see a(1) and a(2) in Fig. 10), and the amount of electricity generated from BIPBs tends to increase (see b(1), b(2), c(1), c(2), d(1), and d(2) in Fig. 10). This occurs because of the increase in heat gain from solar radiation [52]. Meanwhile, as the orientation changes from west (W) to south (S) or from east (E) to south (S), both cooling energy demand and the amount of electricity generated by BIPBs tend to decline. This happens because the heat gain from solar radiation is reduced. In other words, since Busan is located in the southern part of South Korea (at a latitude of 37.3°), the daily solar altitude during the summer ranges from 0° to 76.20° (= 90° − 37.3° + 23.5°). Accordingly, where a building faces south, the summer sunlight cannot enter the building at noon (leading to a reduction in cooling energy demand). In addition, there is an increase in shading effect (leading to a reduction in electricity generated from BIPBs).
- *WWR (η: y axis)*: In general, the U-value of the window and its solar heat gain coefficient are greater than those of the wall. Accordingly, as the WWR increases, the heat loss caused by heat transmission increases (leading to a reduction in cooling energy demand), and the heat gain attributable to radiation also increases (leading to an increase in cooling energy demand, but also to an increase in electricity generated by BIPBs). As a result, in every orientation, as the WWR increases, the cooling demand sharply increases (see a(1) and a(2) in Fig. 10), and the amount of electricity generated from BIPBs sharply increases (see b(1), b(2), c(1), c(2), d(1), and d(2) in Fig. 10). Meanwhile, in the north (N) of the country, the changes appear to be very small.

3.2. Validation of the developed model

This study assessed the feasibility of the developed model ('i-FEM') through the validation process in two ways: (i) efficiency (i.e., computational time) and (ii) effectiveness (i.e., prediction accuracy). First, the model efficiency was adopted to evaluate whether the usability of the developed model was enhanced by simplifying the complex process of the conventional methods. Second, the model effectiveness was adopted to evaluate whether the integrity of the developed model was achieved by simultaneously analyzing various aspects of the BEDS.

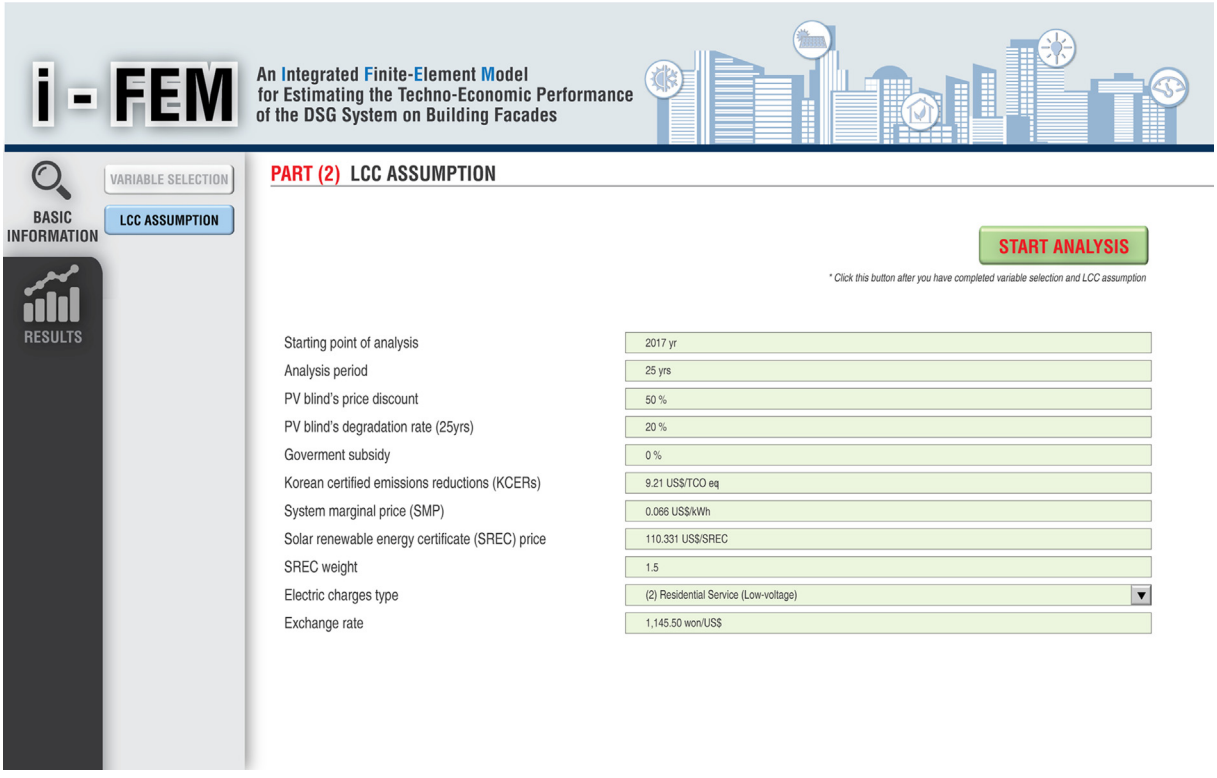

Fig. 6. Graphic user interface of the i-FEM Part 2: LCC assumption.

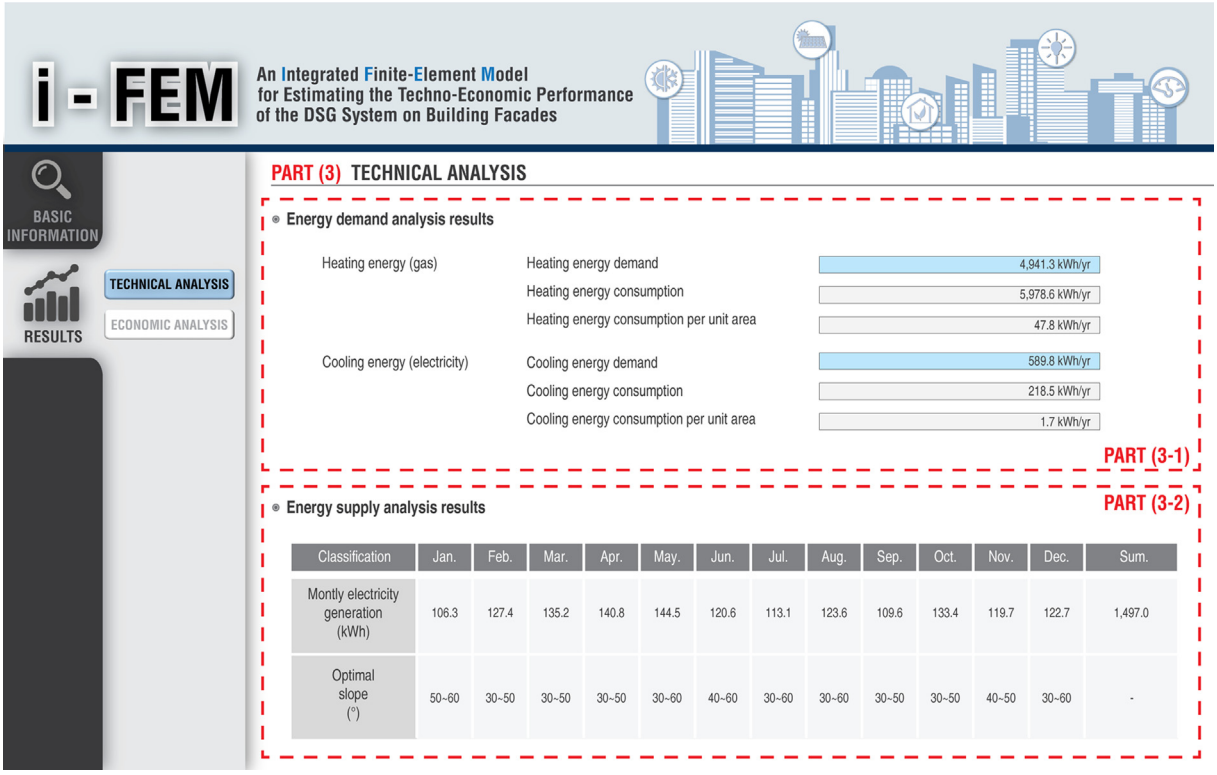
i - FEM
An Integrated Finite-Element Model for Estimating the Techno-Economic Performance of the DSG System on Building Facades
BASIC INFORMATION
RESULTS
TECHNICAL ANALYSIS
ECONOMIC ANALYSIS
PART (3) TECHNICAL ANALYSIS
Energy demand analysis results
Heating energy (gas)
Heating energy demand 4,941.3 kWh/yr
Heating energy consumption 5,978.6 kWh/yr
Heating energy consumption per unit area 47.8 kWh/yr
Cooling energy (electricity)
Cooling energy demand 589.8 kWh/yr
Cooling energy consumption 218.5 kWh/yr
Cooling energy consumption per unit area 1.7 kWh/yr
PART (3-1)
Energy supply analysis results
PART (3-2)
Classification Jan. Feb. Mar. Apr. May. Jun. Jul. Aug. Sep. Oct. Nov. Dec. Sum.
Montly electricity generation (kWh) 106.3 127.4 135.2 140.8 144.5 120.6 113.1 123.6 109.6 133.4 119.7 122.7 1,497.0
Optimal slope (°) 50~60 30~50 30~50 30~50 30~60 40~60 30~60 30~60 30~50 30~50 40~50 30~60 -

Fig. 7. Graphic user interface of the i-FEM Part 3: Technical analysis.

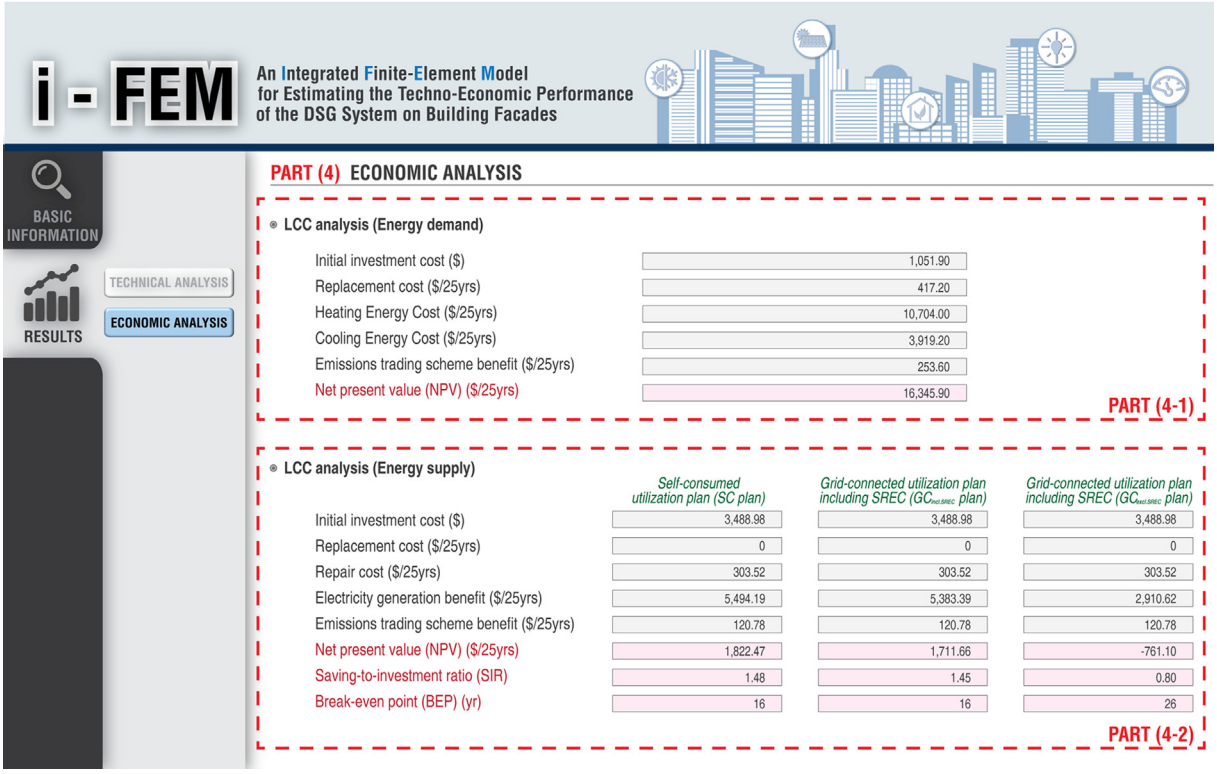
i - FEM
An Integrated Finite-Element Model for Estimating the Techno-Economic Performance of the DSG System on Building Facades
BASIC INFORMATION
RESULTS
TECHNICAL ANALYSIS
ECONOMIC ANALYSIS
PART (4) ECONOMIC ANALYSIS
LCC analysis (Energy demand)
Initial investment cost ($) 1,051.90
Replacement cost ($/25yrs) 417.20
Heating Energy Cost ($/25yrs) 10,704.00
Cooling Energy Cost ($/25yrs) 3,919.20
Emissions trading scheme benefit ($/25yrs) 253.60
Net present value (NPV) ($/25yrs) 16,345.90
PART (4-1)
LCC analysis (Energy supply)
Self-consumed utilization plan (SC plan)
Grid-connected utilization plan including SREC (GC incl.SREC plan)
Grid-connected utilization plan including SREC (GC incl.SREC plan)
Initial investment cost ($) 3,488.98 3,488.98 3,488.98
Replacement cost ($/25yrs) 0 0 0
Repair cost ($/25yrs) 303.52 303.52 303.52
Electricity generation benefit ($/25yrs) 5,494.19 5,383.39 2,910.62
Emissions trading scheme benefit ($/25yrs) 120.78 120.78 120.78
Net present value (NPV) ($/25yrs) 1,822.47 1,711.66 -761.10
Saving-to-investment ratio (SIR) 1.48 1.45 0.80
Break-even point (BEP) (yr) 16 16 26
PART (4-2)

Fig. 8. Graphic user interface of the i-FEM Part 4: Economic analysis.

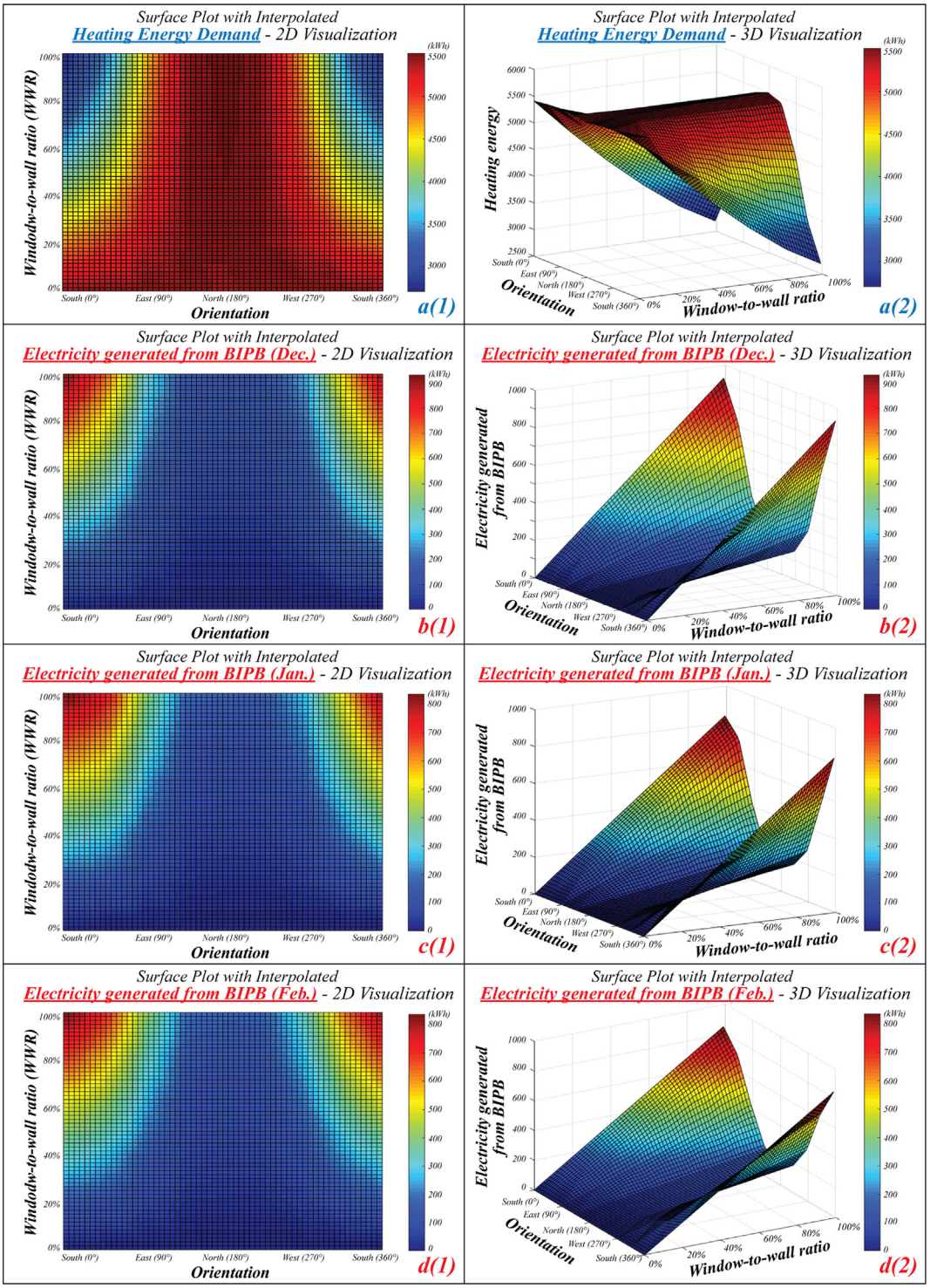

Fig. 9. Nonlinearity analysis between the heating energy demand and the amount of electricity generated from BIPB in the winter season (December, January and February).

3.2.1. Model efficiency

To evaluate the efficiency of the developed model (i-FEM), this study measured the computational time required for estimating the techno-economic performance of the DSG system. As explained in Section 2.5, the integrated model was developed to simplify the complex process of the conventional approach while analyzing energy demand and supply. Thus, the integrated model can be used by simply entering information on the key design variables. In other words, there is no need to carry out the complex process of the conventional approach (e.g., data collection via detailed drawings and specifications,

energy simulation modeling, repetitive communication with the experts in the field of building energy demand and supply, and cost-benefit analysis). This study measured the computational time required for estimating the techno-economic performance of the DSG system after entering the relevant information. It was found that the computational process on a computer (*Processor, Intel® Core™ i7-6700 CPU @ 3.40 GHz; RAM, 32.0 GB available*) could be completed in only 6 s. As a result, the usability of the newly developed integrated model (i-FEM) was validated in terms of the computational time.

3.2.2. Model effectiveness

To evaluate the effectiveness of the developed model (i-FEM), this study measured the prediction accuracy by comparing the estimated values taken from the developed model with the values taken from energy simulation modeling such as '*DesignBuilder v3.0*' and '*Autodesk Ecotect analysis*' software programs. As an evaluation measure, the mean absolute percentage error (MAPE) was adopted (see Eq. (4)). The results were summarized in two ways (for the BED and the BES).

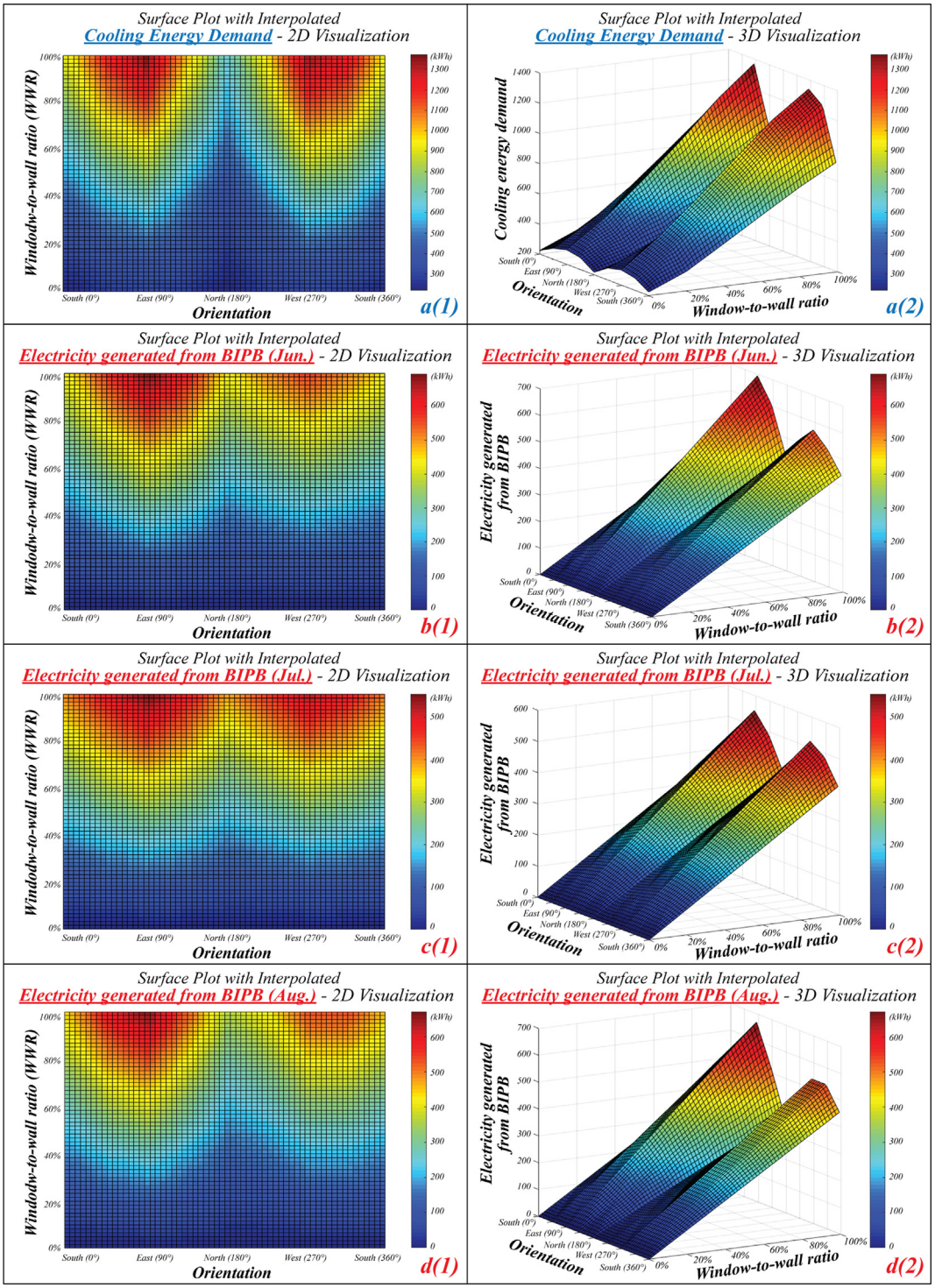

Fig. 10. Nonlinearity analysis between the cooling energy demand and the amount of electricity generated from BIPB during the summer season (June, July and August).

Table 4
Validation of prediction accuracy in terms of the heating energy demand.

Orientation (°)	Household location	[a]MAPE (%) Window-to-wall ratio (WWR) (%)				
		10	30	50	70	90
22.5	Top floor-inside	0.03	0.92	1.32	2.30	3.63
	Top floor-outside	0.01	0.79	1.16	2.01	3.18
	Middle floor-inside	0.05	1.23	1.75	3.01	4.54
	Middle floor-outside	0.00	1.05	1.51	2.60	4.10
	Lowest floor-inside	0.01	1.01	1.43	2.45	3.98
	Lowest floor-outside	0.06	0.88	1.25	2.15	3.43
67.5	Top floor-inside	0.04	0.57	0.75	1.25	1.87
	Top floor-outside	0.06	0.50	0.63	1.06	1.65
	Middle floor-inside	0.03	0.76	1.08	1.70	2.59
	Middle floor-outside	0.07	0.65	0.89	1.48	2.20
	Lowest floor-inside	0.00	0.65	0.89	1.52	2.25
	Lowest floor-outside	0.05	0.55	0.76	1.28	1.94
112.5	Top floor-inside	0.13	0.08	0.03	0.06	0.12
	Top floor-outside	0.09	0.13	0.04	0.14	0.21
	Middle floor-inside	0.18	0.07	0.06	0.01	0.07
	Middle floor-outside	0.11	0.14	0.03	0.12	0.17
	Lowest floor-inside	0.10	0.11	0.00	0.17	0.22
	Lowest floor-outside	0.06	0.17	0.07	0.23	0.31
157.5	Top floor-inside	0.14	0.07	0.21	0.16	0.20
	Top floor-outside	0.13	0.06	0.20	0.14	0.18
	Middle floor-inside	0.17	0.08	0.26	0.21	0.26
	Middle floor-outside	0.15	0.07	0.23	0.18	0.24
	Lowest floor-inside	0.15	0.03	0.19	0.16	0.22
	Lowest floor-outside	0.15	0.02	0.18	0.13	0.18
202.5	Top floor-inside	0.14	0.39	0.36	0.59	0.74
	Top floor-outside	0.10	0.34	0.31	0.51	0.64
	Middle floor-inside	0.19	0.50	0.50	0.78	0.98
	Middle floor-outside	0.14	0.42	0.41	0.66	0.83
	Lowest floor-inside	0.10	0.39	0.41	0.63	0.74
	Lowest floor-outside	0.06	0.34	0.33	0.54	0.66
247.5	Top floor-inside	0.28	0.49	0.85	1.01	1.32
	Top floor-outside	0.30	0.48	0.85	1.00	1.27
	Middle floor-inside	0.35	0.61	1.03	1.34	1.78
	Middle floor-outside	0.35	0.59	1.02	1.26	1.65
	Lowest floor-inside	0.32	0.55	1.04	1.27	1.54
	Lowest floor-outside	0.32	0.55	1.01	1.22	1.48
292.5	Top floor-inside	0.45	0.58	1.26	1.55	1.70
	Top floor-outside	0.39	0.48	1.09	1.32	1.42
	Middle floor-inside	0.56	0.75	1.55	1.93	2.18
	Middle floor-outside	0.47	0.62	1.36	1.63	1.85
	Lowest floor-inside	0.45	0.60	1.37	1.71	1.90
	Lowest floor-outside	0.37	0.49	1.18	1.46	1.59
337.5	Top floor-inside	0.07	1.50	2.34	3.95	5.86
	Top floor-outside	0.01	1.32	2.04	3.40	5.11
	Middle floor-inside	0.16	1.73	2.78	4.60	6.71
	Middle floor-outside	0.10	1.48	2.40	3.97	5.84
	Lowest floor-inside	0.11	1.27	2.06	3.38	5.10
	Lowest floor-outside	0.06	1.12	1.81	2.94	4.45
Yearly-based MAPE (%)		1.01				

Note: The validation process was conducted under the following conditions (i.e. the southern part of the region, Type 5 (125 m^2) of the household type, (Clr5 + Air6 + Clr5) & (Clr5 + Air6 + Clr5), and the awning type was none).
[a] *MAPE* stands for mean absolute percentage error.

$$f_{MAPE} = \left(\sum_{i=1}^{n} \left| \frac{SV^i - EV^i}{SV^i} \right| \times \frac{1}{n} \right) \times 100 \quad (4)$$

where f_{MAPE} stands for the mean absolute percentage error; SV stands for simulated values; EV stands for estimated values via the i-FEM; and n stands for the number of data (month).

- *Prediction accuracy for the BED:* The midpoints of two design variables (which was used to develop the finite element mesh for the BED, for which see Section 2.3) were used in the validation process as follows: (i) orientation (ξ): 22.5°, 67.5°, 112.5°, 157.5°, 202.5°, 247.5°, 292.5°, and 337.5°; and (ii) WWR (η): 10%, 30%, 50%, 70%, and 90%. Table 4 and SD Table S7 show the prediction accuracy (i.e., the annual average MAPE) for the heating energy demand (1.01%) and the cooling energy demand (9.27%), respectively.
- *Prediction accuracy for the BES:* The midpoints of two design variables (which was used to develop the finite element mesh for the BES, for which see Section 2.3) were used in the validation process as follows: (i) orientation (ξ): 22.5°, 67.5°, 112.5°, 157.5°, 202.5°, 247.5°, 292.5°, and 337.5°; and (ii) VT (η): 35%, 45%, 55%, 65%, and 75%. Table 5 shows the prediction accuracy (i.e., the annual average MAPE) for the building energy supply (3.55%) within a range of 1.87% (September) to 6.26% (December).

As a result, the integrity of the newly developed integrated model (i-FEM) was validated in terms of the prediction accuracy.

3.3. Practical application

The practical application of the develop model (i-FEM) to the 'S' apartment block in South Korea was conducted for potential users to understand how to implement the developed model in a clear way. It was tested under these conditions: southern region, 302° south-western orientation, 125 m^2 floorplan (Type 5), middle floor outside (household location), 71.5 m^2 (exterior wall area), 32.4% (WWR), 23.17 m^2 (exterior window area), (Clr6 + Air12 + Clr6) (glazing type), and 62.3% (VT). In addition, some factors were assumed to relate to the DSG system (i.e. venetian blind, 100% window-to-PV panel ratio, CIGS (PV panel), and PV panel efficiency of 11.7%). The results of the practical application can be summarized as follows: (i) technical analysis and (ii) economic analysis.

3.3.1. Technical analysis

Using the aforementioned information, the technical analysis for the practical application can be summarized in two ways (for the BED and the BES).

- *Technical analysis for the BED:* Two design variables, orientation (ξ): 302° and WWR (η): 32.4%, were determined to estimate the heating and cooling energy demand via the FEM. For the heating energy demand, the nine extreme points were generated with the following values: (i) orientation (ξ_n: 270°, ξ_{n+1}: 315°, ξ_{n+2}: 360°) and (ii) WWR (η_n: 20%, η_{n+1}: 40%, η_{n+2}: 60%). In other words, the nine extreme points were determined as follows: ϕ_1 (ξ_1: 270°, η_1: 20%) = 5442.1kWh/yr; ϕ_2 (ξ_1: 270°, η_2: 40%) = 5181.4 kWh/yr; ϕ_3 (ξ_1: 270°, η_3: 60%) = 4950.5kWh/yr; ϕ_4 (ξ_2: 315°, η_1: 20%) = 5160.5kWh/yr; ϕ_5 (ξ_2: 315°, η_2: 40%) = 4639.1kWh/yr; ϕ_6 (ξ_2: 315°, η_3: 60%) = 4168.7 kWh/yr; ϕ_7 (ξ_3: 360°, η_1: 20%) = 4989.5kWh/yr; ϕ_8 (ξ_3: 360°, η_2: 40%) = 4320.8kWh/yr; and ϕ_9 (ξ_3: 360°, η_3: 60%) = 3715.8kWh/yr (see Fig. 11). The nine polynomial expressions were set up using the nine extreme points (see Eq. (5)). Then, the interpolation function was determined through the inverse matrix (see Eqs. (6) and (7)). Finally, the heating energy demand was estimated at 4,941.3 kWh/yr (see Eq. (8)). Following the aforementioned process, the cooling energy demand was estimated at 589.8 kWh/yr (see SD Equations (S6)-(S9)). Thereafter, the values of the energy demand were converted into the values of the energy consumption (heating 5978.6 kWh/yr and cooling 218.5 kWh/yr respectively) by taking account of the coefficients of performance for the equipment (heating 0.83 and cooling 2.70).

- *Technical analysis for the BES:* Two design variables, orientation (ξ): 302° and VT (η): 62.3%, were determined to estimate the amount of electricity generated from BIPBs via the FEM. For electricity generation in January, the nine extreme points were calculated with the following values: (i) orientation (ξ_n: 270°, ξ_{n+1}: 315°, ξ_{n+2}: 360°) and (ii) VT (η_n: 50%, η_{n+1}: 60%, η_{n+2}: 70%). In other words, the nine extreme points were determined as follows: ϕ_1 (ξ_1: 270°, η_1: 50%) = 54.4 kWh/yr; ϕ_2 (ξ_1: 270°, η_2: 60%) = 60.0 kWh/yr; ϕ_3 (ξ_1: 270°, η_3: 70%) = 64.8 kWh/yr; ϕ_4 (ξ_2: 315°, η_1: 50%) = 115.7 kWh/yr; ϕ_5 (ξ_2: 315°, η_2: 60%) = 123.3 kWh/yr; ϕ_6 (ξ_2: 315°, η_3: 70%) = 129.8 kWh/yr; ϕ_7 (ξ_3: 360°, η_1: 50%) = 177.3 kWh/yr; ϕ_8 (ξ_3: 360°, η_2: 60%) = 187.7 kWh/yr; and ϕ_9 (ξ_3: 360°, η_3: 70%) = 196.7 kWh/yr (see Fig. 12). The nine polynomial expressions were set up using the nine extreme points (see Eq. (9)). Then, the interpolation function was determined through the inverse matrix (see Eqs. (10) and (11)). Finally, the amount of electricity generated from BIPBs in January was calculated at 106.3 kWh/yr (see Eq. (12)). According to the similar process described above, the annual amount of electricity generated by BIPBs was calculated at 1,497.0 kWh/yr (see SD Equations (S6) to (S9)). SD Table S8 shows the details of the coefficient of variables by FEM model, together with the monthly amount of electricity generated from BIPBs and the relevant estimated results.

3.3.2. Economic analysis results

Based on the technical analysis, the economic viability for the practical application can be analyzed by considering the utilization plan (SC plan, $GC_{incl.SREC}$ plan, and $GC_{excl.SREC}$ plan) as well as the life-cycle cost (see Table 6). First, for the NPV, the SC plan (US$ 1822.5) was deemed almost equal to the $GC_{incl.SREC}$ plan (US$ 1711.7) and superior

Table 5
Validation of prediction accuracy in terms of the building energy supply.

Orientation (°)	[a]VT (%)	[b]MAPE (%)											
		January	February	March	April	May	June	July	August	September	October	November	December
22.5	35	4.57	2.71	0.81	5.44	7.93	6.19	6.19	6.69	4.56	1.53	2.86	5.67
	45	3.85	2.25	0.48	2.67	5.34	3.12	3.18	4.19	1.93	1.47	2.12	5.60
	55	3.65	2.21	1.68	2.85	7.26	6.21	5.95	5.57	1.89	0.21	2.67	5.66
	65	3.42	2.61	0.84	2.87	9.58	6.11	4.47	7.09	0.68	0.76	2.98	5.35
	75	3.45	3.38	0.59	2.66	7.55	5.15	3.56	6.20	0.50	0.80	3.57	5.32
67.5	35	6.31	2.78	1.59	0.26	0.90	0.67	0.35	0.05	0.07	3.20	3.87	5.56
	45	7.17	3.09	1.97	1.51	1.71	0.73	1.86	0.75	1.42	3.15	3.71	7.04
	55	5.66	3.00	2.05	1.44	0.06	1.13	0.22	0.10	1.24	2.51	2.96	6.55
	65	5.16	3.45	1.49	1.58	0.15	0.23	0.17	0.13	1.39	2.09	2.24	5.19
	75	2.52	2.72	1.68	2.03	0.87	1.03	1.33	0.73	1.88	2.24	1.67	4.80
112.5	35	3.09	3.03	2.51	3.42	4.65	3.25	3.11	3.83	2.34	2.09	0.29	6.21
	45	7.60	5.81	0.12	1.47	1.58	0.52	0.67	1.11	0.69	1.43	3.97	9.78
	55	9.54	4.74	2.95	3.10	2.10	0.54	0.13	2.65	2.17	0.90	5.87	11.55
	65	4.73	0.23	4.27	3.82	3.06	1.98	2.02	3.90	3.52	4.37	3.94	11.64
	75	2.71	2.43	4.94	4.39	3.70	2.55	2.79	4.33	4.05	5.83	2.42	10.23
157.5	35	8.76	6.44	7.57	8.42	11.55	10.65	11.14	10.66	8.08	4.82	6.88	9.35
	45	5.09	6.31	6.38	4.32	1.83	0.97	0.05	0.65	5.38	8.23	6.71	4.24
	55	3.64	4.42	5.05	5.25	0.32	3.30	2.08	1.97	5.04	6.37	5.20	2.79
	65	0.30	0.40	2.27	1.60	3.69	4.17	3.19	1.60	2.05	3.49	1.25	1.29
	75	1.20	1.98	2.42	1.58	5.50	5.41	4.34	3.19	2.50	4.31	2.95	0.14
202.5	35	6.04	8.22	1.06	3.30	6.85	5.81	4.35	5.57	1.42	5.01	11.54	10.92
	45	7.03	9.91	3.79	1.10	6.34	4.74	3.68	3.99	0.04	7.12	12.53	11.65
	55	6.83	9.71	3.42	2.35	9.15	4.87	4.88	5.58	0.56	6.96	12.10	10.97
	65	7.53	10.06	3.11	2.64	6.85	4.16	2.82	4.17	0.81	7.02	12.52	11.76
	75	8.80	11.09	3.80	2.15	5.67	2.85	1.63	3.13	0.23	7.82	13.53	13.14
247.5	35	0.14	3.04	5.43	3.06	1.01	1.50	0.08	1.93	2.91	5.37	12.14	3.74
	45	2.56	1.83	5.31	1.91	0.35	0.69	0.65	1.36	1.62	4.66	8.47	0.06
	55	2.27	7.10	4.69	0.73	1.03	0.55	0.29	1.17	0.81	8.48	13.21	4.03
	65	4.08	7.12	4.30	0.67	0.74	0.62	0.03	1.27	0.89	6.61	13.06	7.40
	75	4.37	6.03	2.71	0.07	0.11	0.22	0.88	0.43	0.14	4.79	11.50	5.63
292.5	35	0.85	1.50	0.23	1.10	2.71	2.97	1.56	1.18	0.50	1.54	3.03	3.68
	45	0.19	1.64	0.10	0.19	3.45	3.96	2.92	2.33	0.99	0.22	2.67	2.39
	55	0.49	1.80	0.14	0.87	1.62	1.92	1.07	1.04	0.96	0.71	1.48	1.40
	65	1.36	1.55	0.69	3.40	5.38	7.44	6.48	6.14	5.03	0.74	0.33	1.75
	75	0.54	1.45	0.02	1.79	2.16	2.63	2.26	2.21	1.98	1.05	0.23	1.41
337.5	35	3.81	4.54	2.64	3.02	4.47	0.37	2.06	2.66	0.68	2.20	5.52	7.67
	45	3.97	4.91	2.49	0.45	2.17	2.28	2.49	0.11	1.46	1.59	6.46	7.41
	55	4.01	4.67	0.66	1.01	3.41	3.45	4.36	1.26	0.93	0.98	7.34	7.40
	65	4.00	3.92	1.29	0.63	4.22	2.88	2.76	1.95	0.56	1.80	7.30	7.16
	75	4.20	3.96	0.16	0.35	3.65	1.72	1.41	1.19	0.85	1.44	7.19	6.95
Monthly-based MAPE (%)		4.14	4.20	2.44	2.29	3.77	2.99	2.59	2.85	1.87	3.40	5.76	6.26
Yearly-based MAPE (%)		3.55											

Note: The validation process was conducted under the following conditions (i.e. the southern part of the region, 1 m^2 of the exterior window area, 100% of the window-to-PV panel ratio, and 11.70% of the efficiency of the CIGS PV panel).

[a] *VT* stands for the visible transmittance.

[b] *MAPE* stands for the mean absolute percentage error.

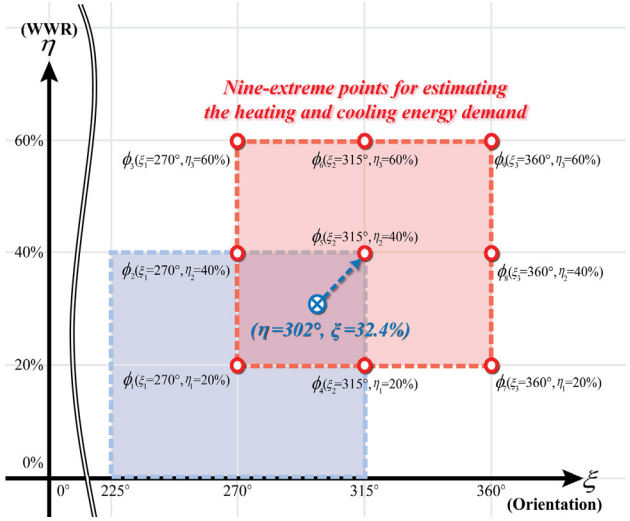

Fig. 11. Nine-extreme points for estimating the heating and cooling energy demand.

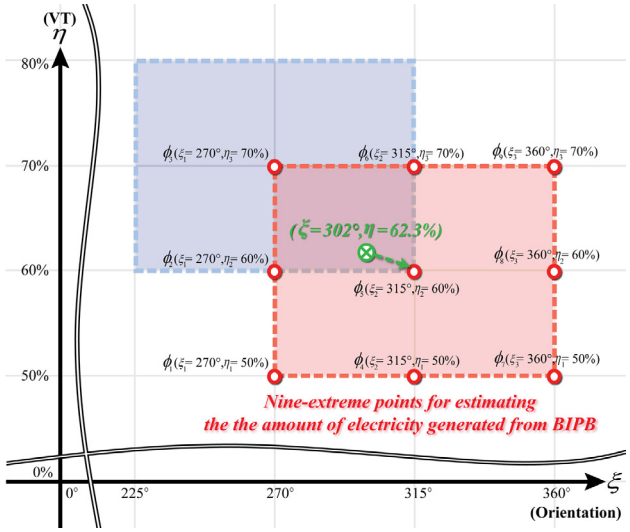

Fig. 12. Nine-extreme points for estimating the amount of electricity generated from BIPBs.

to the $GC_{excl.SREC}$ plan (US$ −761.1). Second, for the SIR, the SC plan (1.48) was deemed almost equal to the $GC_{incl.SREC}$ plan (1.45) and superior to the $GC_{excl.SREC}$ plan (0.80). Third, for the BEP, the 16-year SC plan was deemed equal to the 16-year $GC_{incl.SREC}$ plan and superior to the 26-year $GC_{excl.SREC}$ plan. As a result, should the DSG system be applied to the 'S' apartment block, it is recommended that either the SC plan or the $GC_{incl.SREC}$ plan be implemented as the utilization plan for electricity generated from BIPBs.

3.4. Potential implications

The newly developed integrated model is expected to be beneficial to the practitioners and researchers who are working in the field of the DSG system in the following potential implications (STEEP): (i) social aspect; (ii) technical aspect; (iii) economic aspect; and (iv) and environmental and policy aspect.

- *Social aspect:* In a big city (such as Seoul, Hong Kong), where there are high-rise and high-density buildings with a high slenderness ratio, it is strongly recommended to utilize the building façade areas as well as the rooftop areas in promoting the DSG systems in the building sector [11–15,21].
- *Technical aspect:* It is reported that the two-axis solar tracking systems can significantly increase the amount of electricity generated from the PV systems by 30–45% relative to the fixed-mount systems [53–56]. The novel technology (i.e. automatic tracking system) can contribute to the achievement of net-zero energy buildings with the DSG system.
- *Economic aspect:* The initial costs of the PV systems are continuously decreasing and the relevant power capacity and efficiency are steadily improving. Furthermore, the financial support such as governmental subsidy is being provided to promote the DSG systems in the building sector. In this regard, the economic viability has been considerably improved from the life cycle perspective [42,43,57,58].
- *Environmental and policy aspect:* In accordance with the Paris climate agreement, the mandatory requirement for the implementation of the new and renewable energy systems in buildings has been globally established [44,45,59,60]. For example, the European Union's Renewable energy directive sets a new and renewable energy target of 20% final energy consumption as a whole by 2020; and 27% by 2030. The Korean government also sets a new and renewable energy target of 20% final energy consumption by 2020.

Table 6
Economic analysis results by utilization plan for the practical application.

Classification		Type of utilization plan		
		[a]SC plan	[b]$GC_{incl.SREC}$ plan	[c]$GC_{excl.SREC}$ plan
Cost	[d]IIC	US$ 3489.0	US$ 3489.0	US$ 3489.0
	Repair cost	US$ 303.5	US$ 303.5	US$ 303.5
Benefit	[e]ESB	US$ 5494.2	–	–
	[f]SMP & [g]SREC	–	US$ 5383.4	US$ 2910.6
	[h]KCERs	US$ 120.8	US$ 120.8	US$ 120.8
[i]NPV		US$ 1822.5	US$ 1711.7	US$ (−761.1)
[j]SIR		1.48	1.45	0.80
[k]BEP		16 yrs.	16 yrs.	26 yrs.

Note:
[a] *SC plan* stands for the self-consumed utilization plan.
[b] *$GC_{incl.SREC}$ plan* stands for the grid-connected utilization plan including the SREC.
[c] *$GC_{excl.SREC}$ plan* stands for the gird-connected utilization plan excluding the SREC.
[d] *IIC* stands for the initial investment cost.
[e] *ESB* stands for the electricity-saving benefit.
[f] *SMP* stands for the system marginal price
[g] *SREC* stands for the solar renewable energy certificate.
[h] *KCERs* stands for the Korean certified emissions reductions.
[i] *NPV* stands for the net-present value.
[j] *SIR* stands for the saving-to-investment ratio.
[k] *BEP* stands for the break-even point; and the exchange rate is 1145.50 won to a US$ (as at August 12, 2017).

In response to the local and global requirements and the relevant technical advancements, it is inevitable to implement the DSG system in the building façade areas as well as the rooftop areas. Especially, in big cities of the developed countries, the rooftop PV system couldn't meet the minimum requirements set by the government due to the limited areas. In this case, the façade PV system should be implemented to sufficiently generate the green electricity in an economic and environmental manner. As a result, with the consideration of the five aspects (i.e. social, technical, economic, environmental and policy aspects), it is concluded that the newly developed integrated model could be used for the feasibility study by decision-makers (e.g., construction managers or facility managers) to investigate the potential impact of the DSG system on building façades in a timely and accurate manner.

$$\begin{bmatrix} 270° & (270°)^2 & (270°)^2{\cdot}20\% & (270°)^2{\cdot}(20\%)^2 & 270°{\cdot}(20\%)^2 & (20\%)^2 & 20\% & 270°{\cdot}20\% & 1 \\ 270° & (270°)^2 & (270°)^2{\cdot}40\% & (270°)^2{\cdot}(40\%)^2 & 270°{\cdot}(40\%)^2 & (40\%)^2 & 40\% & 270°{\cdot}40\% & 1 \\ 270° & (270°)^2 & (270°)^2{\cdot}60\% & (270°)^2{\cdot}(60\%)^2 & 270°{\cdot}(60\%)^2 & (60\%)^2 & 60\% & 270°{\cdot}60\% & 1 \\ 315° & (315°)^2 & (315°)^2{\cdot}20\% & (315°)^2{\cdot}(20\%)^2 & 315°{\cdot}(20\%)^2 & (20\%)^2 & 20\% & 315°{\cdot}20\% & 1 \\ 315° & (315°)^2 & (315°)^2{\cdot}40\% & (315°)^2{\cdot}(40\%)^2 & 315°{\cdot}(40\%)^2 & (40\%)^2 & 40\% & 315°{\cdot}40\% & 1 \\ 315° & (315°)^2 & (315°)^2{\cdot}60\% & (315°)^2{\cdot}(60\%)^2 & 315°{\cdot}(60\%)^2 & (60\%)^2 & 60\% & 315°{\cdot}60\% & 1 \\ 360° & (360°)^2 & (360°)^2{\cdot}20\% & (360°)^2{\cdot}(20\%)^2 & 360°{\cdot}(20\%)^2 & (20\%)^2 & 20\% & 360°{\cdot}20\% & 1 \\ 360° & (360°)^2 & (360°)^2{\cdot}40\% & (360°)^2{\cdot}(40\%)^2 & 360°{\cdot}(40\%)^2 & (40\%)^2 & 40\% & 360°{\cdot}40\% & 1 \\ 360° & (360°)^2 & (360°)^2{\cdot}60\% & (360°)^2{\cdot}(60\%)^2 & 360°{\cdot}(60\%)^2 & (60\%)^2 & 60\% & 360°{\cdot}60\% & 1 \end{bmatrix} \begin{bmatrix} \alpha_1 \\ \alpha_2 \\ \alpha_3 \\ \alpha_4 \\ \alpha_5 \\ \alpha_6 \\ \alpha_7 \\ \alpha_8 \\ \alpha_9 \end{bmatrix} = \begin{bmatrix} 5442.1 \\ 5181.4 \\ 4950.5 \\ 5160.5 \\ 4639.1 \\ 4168.7 \\ 4989.5 \\ 4320.8 \\ 3715.8 \end{bmatrix} \tag{5}$$

$$\begin{bmatrix} \alpha_1 \\ \alpha_2 \\ \alpha_3 \\ \alpha_4 \\ \alpha_5 \\ \alpha_6 \\ \alpha_7 \\ \alpha_8 \\ \alpha_9 \end{bmatrix} = \begin{bmatrix} 270° & (270°)^2 & (270°)^2{\cdot}20\% & (270°)^2{\cdot}(20\%)^2 & 270°{\cdot}(20\%)^2 & (20\%)^2 & 20\% & 270°{\cdot}20\% & 1 \\ 270° & (270°)^2 & (270°)^2{\cdot}40\% & (270°)^2{\cdot}(40\%)^2 & 270°{\cdot}(40\%)^2 & (40\%)^2 & 40\% & 270°{\cdot}40\% & 1 \\ 270° & (270°)^2 & (270°)^2{\cdot}60\% & (270°)^2{\cdot}(60\%)^2 & 270°{\cdot}(60\%)^2 & (60\%)^2 & 60\% & 270°{\cdot}60\% & 1 \\ 315° & (315°)^2 & (315°)^2{\cdot}20\% & (315°)^2{\cdot}(20\%)^2 & 315°{\cdot}(20\%)^2 & (20\%)^2 & 20\% & 315°{\cdot}20\% & 1 \\ 315° & (315°)^2 & (315°)^2{\cdot}40\% & (315°)^2{\cdot}(40\%)^2 & 315°{\cdot}(40\%)^2 & (40\%)^2 & 40\% & 315°{\cdot}40\% & 1 \\ 315° & (315°)^2 & (315°)^2{\cdot}60\% & (315°)^2{\cdot}(60\%)^2 & 315°{\cdot}(60\%)^2 & (60\%)^2 & 60\% & 315°{\cdot}60\% & 1 \\ 360° & (360°)^2 & (360°)^2{\cdot}20\% & (360°)^2{\cdot}(20\%)^2 & 360°{\cdot}(20\%)^2 & (20\%)^2 & 20\% & 360°{\cdot}20\% & 1 \\ 360° & (360°)^2 & (360°)^2{\cdot}40\% & (360°)^2{\cdot}(40\%)^2 & 360°{\cdot}(40\%)^2 & (40\%)^2 & 40\% & 360°{\cdot}40\% & 1 \\ 360° & (360°)^2 & (360°)^2{\cdot}60\% & (360°)^2{\cdot}(60\%)^2 & 360°{\cdot}(60\%)^2 & (60\%)^2 & 60\% & 360°{\cdot}60\% & 1 \end{bmatrix}^{-1} \begin{bmatrix} 5442.1 \\ 5181.4 \\ 4950.5 \\ 5160.5 \\ 4639.1 \\ 4168.7 \\ 4989.5 \\ 4320.8 \\ 3715.8 \end{bmatrix} \tag{6}$$

$$\phi(\xi, \eta) = 1.60{\cdot}\xi - 0.003{\cdot}\xi^2 + 0.16{\cdot}\xi^2{\cdot}\eta - 0.03{\cdot}\xi^2{\cdot}\eta^2 + 21.05{\cdot}\xi{\cdot}\eta^2 - 3422.19{\cdot}\eta^2 + 20470.76{\cdot}\eta - 123.45{\cdot}{\cdot}\eta + 5498.69 \tag{7}$$

$$\begin{aligned} \phi(302°, 32.4\%) = {} & 1.60{\cdot}302° - 0.003{\cdot}(302°)^2 + 0.16{\cdot}(302°)^2{\cdot}32.4\% \\ & - 0.03{\cdot}(302°)^2{\cdot}(32.4\%)^2 + 21.05{\cdot}302°{\cdot}(32.4\%)^2 \\ & - 3422.19{\cdot}(32.4\%)^2 + 20470.76{\cdot}32.4\% - 123.45{\cdot}302°{\cdot}32.4\% \\ & + 5498.69 = 4941.3 \end{aligned} \tag{8}$$

where ϕ stands for the heating energy demand; ξ stands for the orientation, η stands for the WWR; and α_1–α_9 stands for the coefficient of the nine-node-based *Lagrangian* shape function.

$$\begin{bmatrix} 270° & (270°)^2 & (270°)^2{\cdot}50\% & (270°)^2{\cdot}(50\%)^2 & 270°{\cdot}(50\%)^2 & (50\%)^2 & 50\% & 270°{\cdot}50\% & 1 \\ 270° & (270°)^2 & (270°)^2{\cdot}60\% & (270°)^2{\cdot}(60\%)^2 & 270°{\cdot}(60\%)^2 & (60\%)^2 & 60\% & 270°{\cdot}60\% & 1 \\ 270° & (270°)^2 & (270°)^2{\cdot}70\% & (270°)^2{\cdot}(70\%)^2 & 270°{\cdot}(70\%)^2 & (70\%)^2 & 70\% & 270°{\cdot}70\% & 1 \\ 315° & (315°)^2 & (315°)^2{\cdot}50\% & (315°)^2{\cdot}(50\%)^2 & 315°{\cdot}(50\%)^2 & (50\%)^2 & 50\% & 315°{\cdot}50\% & 1 \\ 315° & (315°)^2 & (315°)^2{\cdot}60\% & (315°)^2{\cdot}(60\%)^2 & 315°{\cdot}(60\%)^2 & (60\%)^2 & 60\% & 315°{\cdot}60\% & 1 \\ 315° & (315°)^2 & (315°)^2{\cdot}70\% & (315°)^2{\cdot}(70\%)^2 & 315°{\cdot}(70\%)^2 & (70\%)^2 & 70\% & 315°{\cdot}70\% & 1 \\ 360° & (360°)^2 & (360°)^2{\cdot}50\% & (360°)^2{\cdot}(50\%)^2 & 360°{\cdot}(50\%)^2 & (50\%)^2 & 50\% & 360°{\cdot}50\% & 1 \\ 360° & (360°)^2 & (360°)^2{\cdot}60\% & (360°)^2{\cdot}(60\%)^2 & 360°{\cdot}(60\%)^2 & (60\%)^2 & 60\% & 360°{\cdot}60\% & 1 \\ 360° & (360°)^2 & (360°)^2{\cdot}70\% & (360°)^2{\cdot}(70\%)^2 & 360°{\cdot}(70\%)^2 & (70\%)^2 & 70\% & 360°{\cdot}70\% & 1 \end{bmatrix} \begin{bmatrix} \alpha_1 \\ \alpha_2 \\ \alpha_3 \\ \alpha_4 \\ \alpha_5 \\ \alpha_6 \\ \alpha_7 \\ \alpha_8 \\ \alpha_9 \end{bmatrix} = \begin{bmatrix} 54.5 \\ 60.0 \\ 64.8 \\ 115.7 \\ 123.3 \\ 129.8 \\ 177.3 \\ 187.7 \\ 196.7 \end{bmatrix} \tag{9}$$

$$\begin{bmatrix} \alpha_1 \\ \alpha_2 \\ \alpha_3 \\ \alpha_4 \\ \alpha_5 \\ \alpha_6 \\ \alpha_7 \\ \alpha_8 \\ \alpha_9 \end{bmatrix} = \begin{bmatrix} 270° & (270°)^2 & (270°)^2{\cdot}50\% & (270°)^2{\cdot}(50\%)^2 & 270°{\cdot}(50\%)^2 & (50\%)^2 & 50\% & 270°{\cdot}50\% & 1 \\ 270° & (270°)^2 & (270°)^2{\cdot}60\% & (270°)^2{\cdot}(60\%)^2 & 270°{\cdot}(60\%)^2 & (60\%)^2 & 60\% & 270°{\cdot}60\% & 1 \\ 270° & (270°)^2 & (270°)^2{\cdot}70\% & (270°)^2{\cdot}(70\%)^2 & 270°{\cdot}(70\%)^2 & (70\%)^2 & 70\% & 270°{\cdot}70\% & 1 \\ 315° & (315°)^2 & (315°)^2{\cdot}50\% & (315°)^2{\cdot}(50\%)^2 & 315°{\cdot}(50\%)^2 & (50\%)^2 & 50\% & 315°{\cdot}50\% & 1 \\ 315° & (315°)^2 & (315°)^2{\cdot}60\% & (315°)^2{\cdot}(60\%)^2 & 315°{\cdot}(60\%)^2 & (60\%)^2 & 60\% & 315°{\cdot}60\% & 1 \\ 315° & (315°)^2 & (315°)^2{\cdot}70\% & (315°)^2{\cdot}(70\%)^2 & 315°{\cdot}(70\%)^2 & (70\%)^2 & 70\% & 315°{\cdot}70\% & 1 \\ 360° & (360°)^2 & (360°)^2{\cdot}50\% & (360°)^2{\cdot}(50\%)^2 & 360°{\cdot}(50\%)^2 & (50\%)^2 & 50\% & 360°{\cdot}50\% & 1 \\ 360° & (360°)^2 & (360°)^2{\cdot}60\% & (360°)^2{\cdot}(60\%)^2 & 360°{\cdot}(60\%)^2 & (60\%)^2 & 60\% & 360°{\cdot}60\% & 1 \\ 360° & (360°)^2 & (360°)^2{\cdot}70\% & (360°)^2{\cdot}(70\%)^2 & 360°{\cdot}(70\%)^2 & (70\%)^2 & 70\% & 360°{\cdot}70\% & 1 \end{bmatrix}^{-1} \begin{bmatrix} 54.5 \\ 60.0 \\ 64.8 \\ 115.7 \\ 123.3 \\ 129.8 \\ 177.3 \\ 187.7 \\ 196.7 \end{bmatrix} \tag{10}$$

$$\phi(\xi, \eta) = 2.14{\cdot}\xi - 0.002{\cdot}(\xi)^2 + 0.005{\cdot}(\xi)^2{\cdot}\eta - 0.002{\cdot}(\xi)^2{\cdot}(\eta)^2 + 1.04{\cdot}\xi{\cdot}(\eta)^2 - 179.54{\cdot}(\eta)^2 + 347.37{\cdot}\eta - 2.14{\cdot}\xi{\cdot}\eta + 438.25 \tag{11}$$

$$\begin{aligned} \phi(302°, 62.3\%) = {} & 2.14{\cdot}302° - 0.002{\cdot}(302°)^2 + 0.005{\cdot}(302°)^2{\cdot}62.3\% \\ & - 0.002{\cdot}(302°)^2{\cdot}(62.3\%)^2 + 1.04{\cdot}302°{\cdot}(62.3\%)^2 \\ & - 179.54{\cdot}(62.3\%)^2 + 347.37{\cdot}62.3\% - 2.14{\cdot}302°{\cdot}62.3\% \\ & + 438.25 = 106.3 \end{aligned} \tag{12}$$

where ϕ stands for the amount of electricity generated from BIPB in January; ξ stands for the orientation, η stands for the VT; and α_1–α_9 stands for the coefficient of the nine-node-based *Lagrangian* shape function.

4. Conclusions

This study developed an integrated model for estimating the techno-economic performance of the DSG system on building façades. The integrated model was developed in five stages: (i) definition of design

variables; (ii) establishment of a standard database; (iii) technical analysis; (iv) economic analysis; and (v) systemization. As a novel approach, the FEM was used to simplify the complex process of the conventional approach, and it was also used to undertake a simultaneous analysis of the building energy demand and supply. In addition, the LCC analysis was conducted to evaluate the economic viability of the DSG system. The main findings of this study can be summarized in three ways.

- *Nonlinearity analysis between energy demand and supply:* It was found that the amount of solar radiation reaching building façades (i.e. heat gain) was significantly dependent upon key design variables which caused seasonal variations, both in the electricity generation from the BIPB and in the heating and cooling energy demand. Additionally, this study demonstrated complex and nonlinear effects of key design variables upon the technical performance of the DSG system.
- *Model validation:* First, in terms of the efficiency (i.e. computational time), it was determined that the integrated model could investigate the techno-economic performance of the DSG system in only 6 s. It means that the usability of the newly developed integrated model (i-FEM) was validated in terms of the computational time. Second, in terms of the effectiveness (i.e., prediction accuracy), it was proved that the integrated model can accurately estimate the technical performance of the DSG system: (i) heating energy demand (1.01%); (ii) cooling energy demand (9.27%); and (iii) building energy supply (3.55%). It means that the integrity of the newly developed integrated model (i-FEM) was validated in terms of the prediction accuracy.
- *Practical application:* The practical application was conducted for the 'S' apartment block in South Korea so as to explain how it can be implemented in practice. The techno-economic performance of the DSG system was estimated as: (i) heating energy demand (5978.6 kWh/yr); (ii) cooling energy demand (218.5 kWh/yr); (iii) electricity generation from BIPBs (1497.0 kWh/yr); and (iv) utilization plan (SC plan) with NPV (US$ 1822.5), SIR (1.48), and BEP (16 years).

It is expected that the newly developed integrated model could be easily used by decision-makers (e.g., construction managers or facility managers) to investigate the techno-economic performance of the DSG system on building façades in a timely and accurate manner. The developed model can be used in the early design stage of a new building (or an existing building) so as to estimate the potential impact of the DSG system on building façade as part of the systematic envelope design process relating to both energy demand and supply.

Meanwhile, the research team plans to extend the model's application. First, the façade PV system will be integrated with the rooftop PV system, in which the shading effects from surrounding buildings can be evaluated by using the GIS. Second, an integrated multi-objective optimization model will be developed so that decision-makers can determine the optimal solution when constrained by limited resources (such as budget allocation, installation area, and minimum requirement for renewable energy). Third, the developed model will be extended to multiple buildings at the community level, which will be connected with the demand response program for peak-load shifting via energy storage or a price-based control strategy.

Acknowledgements

This work was supported by the National Research Foundation of Korea (NRF) grant funded by the Korean government (MSIP; Ministry of Science, ICT & Future Planning) (NRF-2016R1C1B2007941).

Appendix A. Software availability

Name of Software

i-FEM – An **i**ntegrated **F**inite **E**lement **M**odel for estimating the techno-economic performance of the DSG system in a building façade, focused on energy demand and supply.

Developer and Contract address

Jeongyoon Oh, Choongwan Koo, and Taehoon Hong. Department of Architectural Engineering, Kyonggi University, Republic of Korea & Department of Architectural Engineering, Yonsei University, Republic of Korea. The model (**i-FEM**) developed in this study and the related standard database can be obtained free of charge from the corresponding author (cwkoo@kgu.ac.kr).

Year first available

2017

Hardware required

The model (**i-FEM**) can be operated in a PC with multi-core processor. At this time, the model (**i-FEM**) can be operated with the following specifications: (i) Processor *(Intel® Core™ i7-4790 CPU @ 3.60 GHz)*; (ii) RAM *(16.00 GB);* and (iii) System type *(64-bit operating system)*.

Software required

Autodesk® Ecotect® Analysis 2011 (for energy simulation tool)Microsoft Excel-based Visual Basic for Application (for model development)
MATLAB® R2012a (for visualization of the results)

Operating system

Windows 7 Enterprise K

Program language (program size)

Microsoft Excel-based Visual Basic for Application (8.316 MB)

Availability

On application to the corresponding author (cwkoo@kgu.ac.kr). The model will be developed as a web-based system, which will be accessed to the official website. Access to the model (**i-FEM**) will be restricted to the project partners. However, user accounts can be made available to researchers upon request.

Cost

The model (**i-FEM**) is being developed as 'user-friendly' but its cost is not determined at this time.

Appendix B. Supplementary material

Supplementary data associated with this article can be found, in the online version, at http://dx.doi.org/10.1016/j.apenergy.2018.06.119.

References

[1] Ministry of Environment (ME). The Paris agreement guideline; 2016.
[2] Ministry of Strategy and Finance (MOSF). The 1st Basic Plan for Response to Climate Change. Available at < http://www.mosf.go.kr > [March 27, 2017].
[3] Architecture & Urban Research Institute (AURI). Current situation of greenhouse gas emissions in domestic buildings and related policy trends; 2010.
[4] Zhao HX, Magoulès F. A review on the prediction of building energy consumption. Renew Sustain Energy Rev 2012;16(6):3586–92.
[5] Ekici BB, Aksoy UT. Prediction of building energy consumption by using artificial neural networks. Adv Eng Softw 2009;40(5):356–62.
[6] Hong T, Koo C, Kim D, Lee M, Kim J. An estimation methodology for the dynamic operational rating of a new residential building using the advanced case-based reasoning and stochastic approaches. Appl Energy 2015;150:308–22.
[7] National law information center. Standard for building energy-saving design. Available at < http://www.law.go.kr > [March 27, 2017].
[8] Housing Bureau (Seoul). Low-carbon, green-energy building-design guidelines; 2009.
[9] Ministry of Land, Infrastructure and Transport (MOLIT). Standard for the design and performance evaluation of residential green buildings; 2010.
[10] Korea National Environmental Technology Information Center (KONETIC). Trends and prospect for distributed generation technology; 2016.
[11] Yang H, Li Y. Potential of building-integrated photovoltaic applications. Int J Low-Carbon Technol 2007;2(3):250–61.
[12] Electrical and Mechanical Services Department (EMSD). Study on the Potential Applications of Renewable Energy in Hong Kong; 2004.
[13] Hong T, Koo C, Oh J, Jeong K. Nonlinearity analysis of the shading effect on the technical–economic performance of the building-integrated photovoltaic blind. Appl Energy 2016;194:467–80.
[14] Koo C, Hong T, Jeong K, Ban C, Oh J. Development of the smart photovoltaic system blind and its impact on net-zero energy solar buildings using technical-economic-political analyses. Energy 2017;124:382–96.
[15] Park HS, Koo C, Hong T, Oh J, Jeong K. A finite element model for estimating the techno-economic performance of the building-integrated photovoltaic blind. Appl Energy 2016;179:211–27.
[16] Lam JC, Tsang CL, Li DH, Cheung CO. Residential building envelope heat gain and cooling energy requirements. Energy 2005;30(7):933–51.
[17] Huang Y, Niu JL, Chung TM. Study on performance of energy-efficient retrofitting measures on commercial building external walls in cooling-dominant cities. Appl Energy 2013;103:97–108.
[18] Koo C, Park S, Hong T, Park H. An estimation model for the heating and cooling demand of a residential building with a different envelope design using the finite element method. Appl Energy 2014;115:205–15.
[19] Hong T, Kim H, Kwak T. Energy-saving techniques for reducing CO_2 emissions in elementary schools. J Manage Eng 2011;28(1):39–50.
[20] Hong T, Koo C, Park J, Park HS. A GIS (geographic information system)-based optimization model for estimating the electricity generation of the rooftop PV (photovoltaic) system. Energy 2014;65:190–9.
[21] Koo C, Hong T, Oh J, Choi JK. Improving the prediction performance of the finite element model for estimating the technical performance of the distributed generation of solar power system in a building façade. Appl Energy 2018;215:41–53.
[22] Kang S, Hwang T, Kim JT. Theoretical analysis of the blinds integrated photovoltaic modules. Energ Build 2012;46:86–91.
[23] Bahr W. A comprehensive assessment methodology of the building integrated photovoltaic blind system. Energ Build 2014;82:703–8.
[24] Hachem C, Athienitis A, Fazio P. Evaluation of energy supply and demand in solar neighborhood. Energ Build 2012;49:335–47.
[25] Hwang T, Kang S, Kim JT. Optimization of the building integrated photovoltaic system in office buildings—focus on the orientation, inclined angle and installed area. Energ Build 2012;46:92–104.
[26] Chae YT, Kim J, Park H, Shin. Building energy performance evaluation of building integrated photovoltaic (BIPV) window with semi-transparent solar cells. Appl Energy 2014;129:217–27.
[27] Suh D, Chang S. An energy and water resource demand estimation model for multi-family housing complexes in Korea. Energies 2012;5(11):4497–516.
[28] Bojic M, Yik F, Sat P. Influence of thermal insulation position in building envelope on the space cooling of high-rise residential buildings in Hong Kong. Energ Build 2001;33(6):569–81.
[29] Ouyang J, Ge J, Hokao K. Economic analysis of energy-saving renovation measures for urban existing residential buildings in China based on thermal simulation and site investigation. Energ Policy 2009;37(1):140–9.
[30] Siraki AG, Pillay P. Study of optimum tilt angles for solar panels in different latitudes for urban applications. Sol Energy 2012;86(6):1920–8.
[31] Cucchiella F, D'Adamo I. Estimation of the energetic and environmental impacts of a roof-mounted building-integrated photovoltaic systems. Renew Sustain Energy Rev 2012;16(7):5245–59.
[32] Pillai GG, Putrus GA, Georgitsioti T, Pearsall NM. Near-term economic benefits from grid-connected residential PV (photovoltaic) systems. Energy 2014;68:832–43.
[33] Vettorato D, Geneletti D, Zambelli P. Spatial comparison of renewable energy supply and energy demand for low-carbon settlements. Cities 2011;28(6):557–66.
[34] Seo D, Koo C, Hong T. A *Lagrangian* finite element model for estimating the heating and cooling demand of a residential building with a different envelope design. Appl Energy 2015;142:66–79.
[35] Estiri H. Building and household X-factors and energy consumption at the residential sector: a structural equation analysis of the effects of household and building characteristics on the annual energy consumption of US residential buildings. Energ Econ 2014;43:178–84.
[36] Ministry of Land, Transport, and Maritime Affairs (MLTM). Standard for the design and performance evaluation of residential green buildings. Seoul (South Korea): MLTM; 2010.
[37] Eskin N, Türkmen H. Analysis of annual heating and cooling energy requirements for office buildings in different climates in Turkey. Energ Build 2008;40(5):763–73.
[38] Power Korea. Exchange (KPX). Survey on electricity consumption characteristics of home appliances. Seoul (South Korea) 2011.
[39] American Society of Heating. Refrigerating and Air-Conditioning Engineers (ASHRAE). ASHRAE guideline 14-2002. Atlanta: ASHRAE; 2002.
[40] Levolor Window Fashions (LWF). Wood blind specification: New Jersey; 2005.
[41] FreeCleanSolar. Available at < http://www.freecleansolar.com/ > [March 27, 2017].
[42] Oh J, Koo C, Hong T, Jeong K, Lee M. An economic impact analysis of residential progressive electricity tariff in implementing the building-integrated photovoltaic blind. Appl Energy 2017;202:259–74.
[43] Korea Energy Management Corporation (KEMCO). Regional support service. Available at < http://www.knrec.or.kr/business/area_intro.aspx > [March 27, 2017].
[44] Korea Energy Management Corporation (KEMCO). Renewable Portfolio System (RPS): Available at < http://www.knrec.or.kr/business/rps_guide.aspx > [March 27, 2017].
[45] Korea Power Exchange (KPX). REC Trading System. Available at < https://www.kpx.or.kr/eng/contents.do?key=300 > [March 27, 2017].
[46] Lee M, Hong T, Koo C, Kim CJ. A break-even analysis and impact analysis of residential solar photovoltaic systems considering state solar incentives. Technol Econ Dev Econ 2017:1–25.
[47] Bank of Korea (BoK). Economic statistics system. Available at < http://ecos.bok.or.kr/ > [March 27, 2017].
[48] Statistics Korea (SK). Korean statistical information service. Available at < http://kosis.kr/ > [March 27, 2017].
[49] Korean Certified Emission Reductions (KCER). Korea voluntary emission reduction. Available at < http://www.kemco.or.kr/new_eng/pg02/pg02020201.asp/ > [March 27, 2017].
[50] Korea Electric Power Corporation (KEPCO). The electric rates table. Available at < http://home.kepco.co.kr/kepco/main.do > [March 27, 2017].
[51] Korea Energy Management Corporation (KEMCO). Oil conversion tons calculated. Available at < http://bpms.kemco.or.kr/toe/toe/toe_new.aspx > [March 27, 2017].
[52] Wikipedia. Solar altitude. Available at < https://ko.wikipedia.org/wiki/ > [March 27, 2017].
[53] Drury E, Lopez A, Denholm P, Margolis R. Relative performance of tracking versus fixed tilt photovoltaic systems in the USA. Prog Photovol: Res Appl 2013;22(12):1302–15.
[54] Eke R, Senturk A. Performance comparison of a double-axis sun tracking versus fixed PV system. Sol Energy 2012;86:2665–72.
[55] Maatallah T, Alimi SE, Nassrallah SB. Performance modeling and investigation of fixed, single and dual-axis tracking photovoltaic panel in Monastir City, Tunisia. Renew Sustain Energy Rev 2011;15:4053–66.
[56] Gómez-Gil FJ, Wang X, Barnett A. Energy production of photovoltaic systems: fixed, tracking, and concentrating. Renew Sustain Energy Rev 2012;16:306–13.
[57] Koo C, Hong T, Lee M, Kim J. An integrated multi-objective optimization model for determining the optimal solution in implementing the rooftop photovoltaic system. Renew Sustain Energy Rev 2016;57:822–37.
[58] Koo C, Hong T, Park J. Development of the life-cycle economic and environmental assessment model for establishing the optimal implementation strategy of the rooftop photovoltaic system. Technol Econ Dev Econ 2018;24(1):27–47.
[59] European Commission (Energy). Renewable Energy: Available at < https://ec.europa.eu/energy/en/topics/renewable-energy > [April 15, 2018].
[60] Electrical and Mechanical Services Department (EMSD). New & Renewable Energy: Available at < https://www.emsd.gov.hk/en/energy_efficiency/new_renewable_energy > [April 15, 2018].